Extracting Aerosol Parameters for the High Resolution Fly's Eye
Using Bistatic Lidar with Multiple Scattering Corrections

Richard C. Gray
July 2001

Abstract

The High Resolution Fly's Eye (HiRes) detectors measure ultraviolet light generated by the collision of extremely high energy cosmic rays with the atmosphere. These measurements are used to reconstruct the properties of the cosmic ray. In order for these measurements to be useful the optical properties of the atmosphere during each event must be known. These optical properties, such as the transmission of the fluorescence light, depend heavily on nightly variations in the concentration and type of aerosol particles in the air. This paper discusses methods to extract parameters that describe the aerosols using nightly bistatic lidar and monte carlo simulations. These methods first assume that photons are allowed to scatter only once before reaching the detector. The effect that multiply scattered photons have on the signal is determined using a monte carlo simulation. These effects can then be accounted for to determine the actual concentrations of aerosols. An average aerosol content at Dugway Proving grounds will be given.

1 Introduction

The High Resolution Fly's Eye experiment is designed to measure the energy spectrum of the highest energy subatomic particles ever detected. These particles are known as ultra high energy cosmic rays. One aspect of the energy spectrum which is currently under investigation is whether or not it vanishes at a predicted cutoff energy. This cutoff energy is known as the GKZ limit. The GKZ limit was independently proposed by Greisen, Zatsepin, and Kuz'min in 1966 (AbuZayyad, 2000). This idea states that only particles less than $4x10^{19}eV$ should be able to reach the earth without interacting with 3K microwave background radiation (Greisen, 1966). The detection of particles above this limit would indicate sources of high energy particles relatively close to earth. No such sources are known to exist.

This experiment measures fluorescence light produced by the interaction of the high energy cosmic ray with the atmosphere. When one of these high energy particles collides with the atmosphere it generates an Extensive Air Shower (EAS) . An EAS occurs when the primary particle, the cosmic ray, collides with another particle and then forms a number of lower energy secondary particles. These lower energy secondary particles then collide again and form more particles. This process produces a shower of charged particles, primarily electrons, that excite nitrogen molecules in the air and cause them to emit ultra violet fluorescence light. The amount of fluorescence light produced is proportional to the energy of the primary particle (AbuZayyad, 2000).

The HiRes detectors are an array of mirrors that collect and focus the light produced by an EAS. Each mirror is aimed at a different part of the sky and reflects the light it receives into a cluster of 256 photo-multiplier tubes (PMT's). Each cluster of PMTs views a section of solid angle that subtends 14 degrees in elevation and 16 degrees in azimuth. Each tube views approximately 1 degree in solid angle. The mirror only allows the PMT to receive light which propagates toward the detector normal to it's own patch of solid angle. It is therefore possible to calculate the plane in which an EAS developed based on the pointing directions of the tubes that received light. The HiRes1 detector is an array of 22 of these mirrors. They are arranged in a single ring that views 360 degrees in azimuth and 14 degrees in elevation.

The amount of fluorescence light produced by an event is primarily a function of the particle's energy. However, the amount of light measured by the HiRes detectors is also a function of the geometry and on atmospheric conditions during the event. The transmission of this fluorescence light from the EAS through the atmosphere can vary significantly on a nightly or even hourly basis. Daily variations can alter the received signal by as much as 50 percent. It is therefore very important to find a way to characterize the atmosphere while the detectors are operating. This characterization must include a way to quantitatively determine both transmission through the atmosphere and the scattering properties. If the clarity of the atmosphere is unknown the ability to reconstruct the cosmic ray energy with any certainty is compromised.

To simplify the problem at hand we separate the atmosphere into two components. The nitrogen and oxygen component has known optical properties and is mostly stable throughout the year (Martin, 1999). This is said to be the molecular component of the atmosphere. All other particles compose the aerosol component. For example, the aerosols include smog, water droplets, dust, or sand particles. The aerosol component has variable optical properties that can change on an hourly basis. Wind can bring dust particles up from the ground and increase the aerosol content, or precipitation could "flush" the atmosphere and decrease the aerosol content. One night the aerosol component could be non-existent and the atmosphere could be virtually molecular. On the next night aerosols could reduce atmospheric transmission by as much as half. The rest of this paper will assume the molecular portion to be constant and will be concerned with the variable aerosol portion.

1.1 Parameterization of Atmospheric Components

In the above section the classification of molecular and aerosol components was based on differences in stability. However, the two components also tend to drastically differ in both their scattering properties and how they are distributed in the atmosphere. Aerosols tend to be larger in size than molecules. Because of this the angular distribution of scattered light tends to be quite different. Also, the density of aerosol particles decreases more rapidly with height above the ground. These differences require that each component be separately characterized. Such a characterization may be done by determining three parameters for each component.

1. Ground Level Scattering length
2. Vertical Distribution
3. Phase Function

The ground level scattering length X_o is equal to $\frac{1}{\rho\sigma_{scat}}$, where ρ is the number density of particles at ground level and σ_{scat} is the scattering cross section of those particles. While ozone absorption is important in the upper atmosphere, scattering is the dominant cross section at ultra violet wavelengths ($300nm$ - $400nm$) in the lower atmosphere (Sokolsky, 1989). The scattering length tells us the average distance a photon may travel at ground level before scattering. In a multi component atmosphere the total mean scattering length is obtained by summing the scattering length of each component in parallel. For example, if an atmosphere contains two components the total scattering length is given by: $\frac{1}{X_{total}} = \frac{1}{X_1} + \frac{1}{X_2}$. Also, the number of photons in a collimated beam, such as a laser, traveling at ground level can be expressed as $N_o e^{\frac{-d}{\chi_o}}$, where d is the distance traveled. The scattering length generally depends on the wavelength of the radiation. For example, the molecular scattering length is proportional to λ^4 and is approximately 18 kilometers at the wavelength of interest. Also, there is a "standard desert" model which parameterizes the average aerosol content in a desert atmosphere. This model was extracted from the MODTRAN program. In this model the aerosol scattering length is approximately 12 kilometers at $355nm$.

The vertical distribution describes how the density of particles changes with height above the ground. Because the reciprocal of the scattering length is proportional to this density, it changes with height in the same manner. For the molecular component this distribution can be approximated as an exponential decay with distance above the ground. This particular model can be derived using a Boltzmann distribution with the energy of the particles (gravitational potential energy) linear with distance above the ground. This model can also be obtained experimentally using radiosonde data (Martin, 1999). For the molecular component of the atmosphere can be approximated in the lower 10km as an exponential decay has a mean height of 8 to 10 kilometers (Elterman, 1965). The derivation of an exponential distribution assumes all the particles have the same mass. While this assumption is nearly true for molecules it may not be for aerosols. Aerosols are a collection of various types of particles. At the outset we have no reason to believe this exponential model should be sufficient for aerosols. Clouds and haze layers are striking examples of deviation from an exponential distribution. However, in the interests of simplicity and the lack of a better model the exponential is used in aerosol models. The "standard desert" description of the distribution is an exponential with a 1.2 kilometer mean height or scale height.

The phase function describes how the probability of scattering into a specific direction varies with scattering angle. We will define the phase function as the differential scattering cross section normalized to unity over solid angle. This can be determined analytically by modeling particles as dielectric spheres which scatter light through the mechanism of dipole radiation. For particles much smaller than the wavelength of interest ($\lambda = 355nm$), such as those in the molecular component, this calculation is quite straight forward. For circularly or unpolarized light incident on small molecules the phase function is $\frac{3}{16\pi}(1 + cos^2(\theta))$. See the appendix for a derivation and a discussion on the effects of linear polarization.

For larger particles the calculation of the phase function is more complicated. Most aerosols are comparable in size to the wavelength of interest. In this case, the phase function is asymmetric about 90 degree scattering, and is biased toward scattering in the direction of the incident radiation. Calculation of the aerosol phase function is further complicated because the aerosols include particles with a wide distribution in size and type. This distribution is generally unknown and can vary with height above the ground. There are many models available describing possible aerosol phase functions. One such model that I will be referring to is one given by Longtin (Longtin et. al., 1988). This is the phase function that is used in the "standard desert" model. An example of what an aerosol phase function may look like is shown in figure 1.1.

Past, analysis of fluorescence data assumed photons that did not reach the detector after their first interaction were lost (AbuZayyad, 2000). This approximation is valid for light sources located at distances much less than the mean scattering length from the detector. In this approximation, the amount of light scattered from a collimated source into a detector would decrease exponentially with the total path length of the light divided by the interaction length along the path. This feature is consistent with absorption or attenuation. With absorption, a photon is effectively removed from the experiment after a single interaction. In an experiment where scattering is the dominant cross section, such as this one, photons may still affect a measurement after their first interaction. As sources become more distant, greater than or equal to the scattering length, it becomes possible

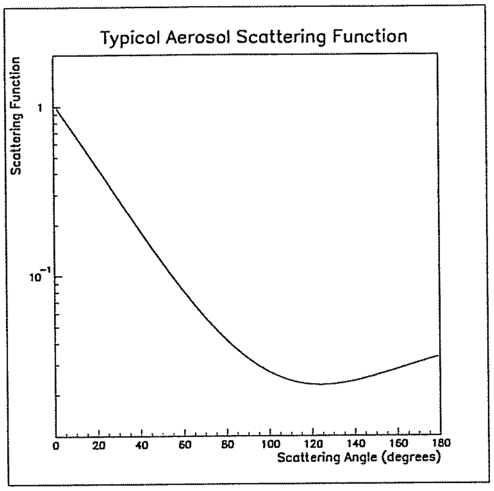

Fig. 1.1: This is a typical aerosol phase function. It comes from a phase function used in a multiple scattering simulation program (MCMSGDS). It is a simple algebraic form intended to approximate the results of Longtin and other researchers. It is shown plotted on a log scale.

for photons that have scattered out of the direction of the incident radiation to scatter one or more times and still be measured. The received signal can be enhanced by multiply scattered photons if there is a non zero time window and angular acceptance when the measurement is made. Multiply scattered photons may have total path lengths which are equal, shorter, or longer than the single scattered photons. Because of this, the enhancement will generally increase as the time window and angular acceptance increases. If only single scattering is considered the analysis of the measurements will overestimate the initial energy of the light source. While calculations that assume single scattering are quite straight forward, the calculations for higher order scattering are more complicated. Figure 1.2 shows a schematic of multiple scattering for a collimated source.

2 Methodology

This section describes the techniques employed to acquire data and to determine aerosol parameters from it. This is done using data from a bi-static lidar and simulation results from a monte carlo program. This lidar consists of a steerable laser system located near the HiRes2 detector and the HiRes1 detector as a receiver (12.6km apart). The laser light is scattered by the atmosphere and this scattered light is measured by HiRes1. The amplitude and distribution of scattered light from the laser can be used to indicate the composition of the atmosphere.

The methods to the extract aerosol parameters use the ratio between the measured signal and the expected signal for a purely molecular atmosphere. This molecular expectation can come from a simulation or from a day with a very low aerosol content. A simulation program called MCMSGDS (Monte Carlo Multiple Scattering General Detector Simulation) is used to give a rough estimate of the percent enhancement caused by multiply scattered photons. This estimate will be used to correct the aerosol parameters extracted from the data.

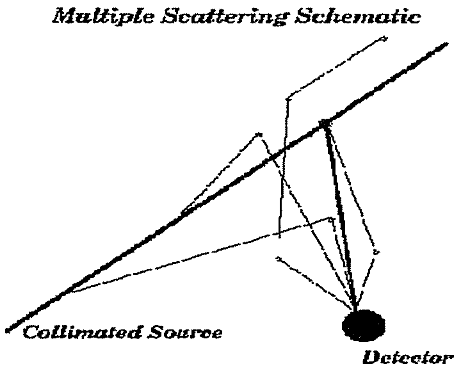

Fig. 1.2: This is a schematic illustrating multiple scattering. The paths taken by four photons which scatter out of the main beam are shown. One photon takes a single scattered path toward the detector while the rest take multiply scattered paths. All reach the detector along a similar direction. The single scatter path is made darker to accentuate it.

2.1 The Bi-static Lidar

LIDAR (Light Detection and Ranging) is often used to study the composition of the atmosphere. A laser is fired into the air at a known geometry. Light scattered by the particles in the atmosphere is received by a detector. The measured signal is analyzed to determine properties of the atmosphere. Most lidar is mono-static, which means that the detector and the laser are located in the same place. This restricts observable scattering angles to 180°, phase functions can therefore not be determined. In this configuration the lidar data is analyzed by looking at how the amplitude of the measured signal varies with time after the initial laser pulse.

This experiment uses a steerable laser located at the site of HiRes2 and the HiRes1 detector as a bi-static lidar. In the bi-static configuration the laser and the detector are separated by a significant distance. In this experiment the laser and the detector are separated by 12.6km. The HiRes cosmic ray detectors consist of an array of stationary mirrors that can instantaneously observe most of the possible scattering angles for a given laser geometry. The HiRes1 detector, with it's 20 mirrors and over 5000 PMTs, is one of the largest optical detectors used in such an experiment.

The HiRes detectors are located at Dugway Proving Grounds in Utah's west desert. They are separated by approximately 12.6 km. The detector involved in the lidar, HiRes1, uses sample and hold electronics and is built on the top of Five-Mile hill. HiRes1 is composed of a ring of twenty-two mirrors. Each mirror focuses light into a cluster of 256 photo-multiplier tubes (PMT's). Each tube views approximately one degree of solid angle. The mirrors each view a patch of solid angle that subtends 14 degrees in elevation and approximately 16 degrees in azimuth. The full ring of mirrors views 360 degrees in azimuth.

The steerable laser system is located by HiRes2 on Camel's Back ridge. The HiRes2 steerable laser system (HR2SLS), is able to point the laser in virtually any direction. The accuracy of it's pointing is better than a tenth of degree in it azimuthal axis and slightly better than that in its elevation axis. The system uses an 8 mJ, 355nm, YAG laser. This laser has been designed to be rugged so it can function properly in the variable weather conditions of Utah's West Desert. The entire system can be remotely operated over a network. Each night the system performs a preprogrammed sequence of shots. In this sequence different optical elements can be placed in the beams path to control the energy and polarization of radiation sent to the sky. The system samples the energy of each shot so that variations in laser energy are known. See figure 2.1.1 for a diagram of the systems components. For a more detailed description of the system see "Steerable Laser System For High Resolution Fly's Eye" by R.J. Mumford ICRC 99 proceedings (Mumford, 1999).

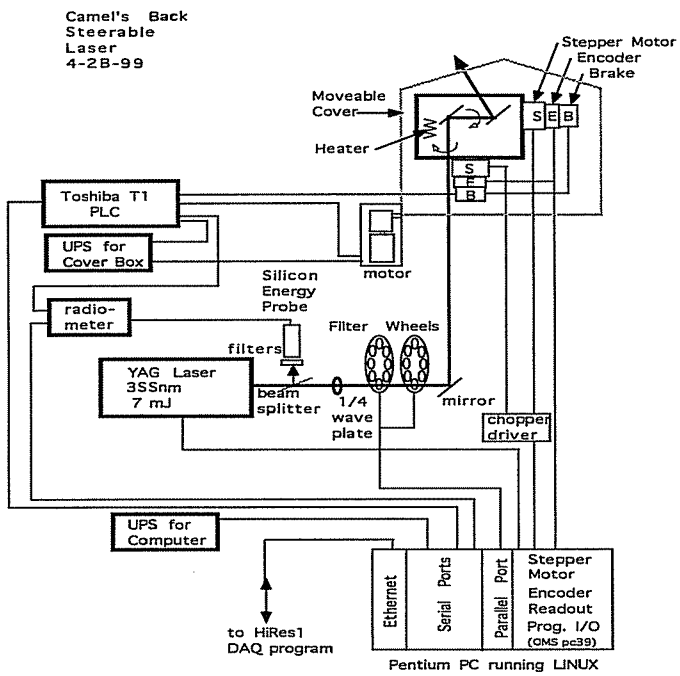

Fig. 2.1.1: This is a diagram of the HiRes2 steerable laser system which, along with the HiRes1 detector, constitutes the bistatic lidar used in this experiment.

2.2 Methods of Extracting Aerosol Parameters

The following methods to extract aerosol parameters use the ratio between the measured data and the expectation for a purely molecular atmosphere. By taking this ratio the effect of the aerosols are isolated. Other than the assumption that the atmosphere possesses horizontal uniformity, the first two methods are independent of specific aerosol models. See "Atmospheric Horizontal Uniformity Measured By a Steerable Laser System At The High Resolution Fly's Eye " by J. R. Mumford for a study of this assumption. These methods assume that the received photons have scattered only once.

The first two methods are orthogonal. By orthogonal I mean that the properties of the atmosphere that affect one of these measurements do not have a significant effect on the other. One measures ground level parameters and is insensitive to how aerosols are distributed throughout the rest of the atmosphere. The other method makes modest assumptions about the aerosol phase function and then tries to determine the vertical distribution independent of the aerosol phase function or ground level scattering length. These methods are independent of specific models. The third method is a global fit. This fit assumes that the aerosols are exponentially decreasing with height and that the phase function is constant with height. This fit alters parameters of this model to minimize the chisquare of all of the measurements. After the global fit has been performed using the single scattering model, approximate multiple scattering corrections based on MCMSGDS will be included.

2.2.1 Orthogonal Measurement of Ground level Parameters

The ground level parameters consist of the ground level aerosol phase function and the ground level mean scattering length. To make this measurement the laser must be steered to a geometry that keeps the propagation of the light as horizontal and as close to the ground as possible. This is because the scattering length increases with height above the ground. These geometries end up being close to the detector and have a wide range of observable scattering angles. The angular distribution of the received signal depends strongly on both the phase function and the scattering length of the aerosols. With this bistatic lidar the phase function and scattering length must be extracted simultaneously. Otherwise, drastic assumptions would have to be made about one or the other. This can be done by simply deriving an expression for the aerosol phase function in terms of the ground level scattering length and the ratio between the observed angular distribution and that predicted for a molecular atmosphere.

We can begin this derivation by writing a simple expression for the angular distribution of measured light from a laser beam in a molecular atmosphere.

$$S_{molec} = E(\theta)\frac{3}{16\pi}(1 + cos^2(\theta)) \tag{1}$$

Here θ is the scattering angle and $\frac{3}{16\pi}(1+cos^2(\theta))$ is the molecular phase function for unpolarized or circularly polarized light obtained by dipole scattering theory. See the appendix for information about the effects of linear polarization. The function $E(\theta)$ contains all other atmospheric effects for the ideal molecular atmosphere along with all geometrical and detector response effects. The next step is to write an expression for the distribution in an atmosphere that does contain aerosols in terms of the $E(\theta)$ function. If the laser light is within the linear response range of the detector it is only necessary to scale the profile by atmospheric effects. The $E(\theta)$ function must be multiplied by the net phase function and scaled by lower atmospheric transmission. First the total ground level phase function should be found. This is done by simply scaling the contribution of each component by it's number density and cross section then adding the scaled phase functions together. Because the ground level scattering length is the reciprocal of the cross section multiplied by particle number density we can scale each phase function in terms of their respective components scattering length. In the case of a two component atmosphere the phase function for component 1 is scaled by $\frac{\frac{1}{X_1}}{\frac{1}{X_1}+\frac{1}{X_2}}$. This allows us to write the total ground level phase function for an atmosphere with an aerosol component as: $(\frac{P(\theta)}{X_a} + \frac{3}{16\pi}\frac{1}{X_m}(1 + cos^2(\theta)))(\frac{1}{\frac{1}{X_a}+\frac{1}{X_m}})$ Here $P(\theta)$ is the normalized aerosol phase function. The aerosol ground level scattering length is X_a and the molecular scattering length is X_m.

Next, it is necessary to scale the expression by the decrease in light received due to atmospheric transmission. This term includes an exponential decay in the signal with total path length divided by the aerosol scattering length. However, with the extra scattering created by the aerosols there is an initial increase in the amount of scattered light. Because of the exponential form for the number of photons in the beam versus distance traveled, we know that the number of photons scattered out of the beam per unit length is proportional to the reciprocal of the scattering length. The function

$E(\theta)$ already took this into account for the molecular atmosphere. So, it is necessary to multiply $E(\theta)$ by the molecular scattering length and then divide by the total scattering length. The total scattering length is found by adding the contribution of each component in parallel. The factor that scales $E(\theta)$ for the increase in scattering is given by: $e^{-\frac{d_1+d_2}{X_a}} X_m(\frac{1}{X_m} + \frac{1}{X_a})$. The distance from the laser to where the light scattered is d_1. The distance from where the light scattered to the detector is given by d_2. It should be noted that not only does this term assume single scattering it is also only valid when the laser geometry is near horizontal.

The angular distribution of measured light in an atmosphere with an aerosol component can be written as:

$$S_{molec+aerosol} = E(\theta)(\frac{P(\theta)}{X_a} + \frac{3}{16\pi}\frac{1}{X_m}(1 + cos^2(\theta)))(\frac{1}{\frac{1}{X_a} + \frac{1}{X_m}})e^{(-\frac{d_1+d_2}{X_a})}(1 + \frac{X_m}{X_a}) \quad (2)$$

The potentially complicated function $E(\theta)$ may be removed by taking the ratio of the two cases.

$$\frac{S_{molec+aerosol}}{S_{molec}} = R(\theta) \quad (3)$$

It is possible to solve for the aerosol phase function in terms of the above ratio.

$$P(\theta) = \frac{3}{16\pi}\frac{X_a}{X_m}(1 + cos^2(\theta))(R(\theta)e^{(\frac{d_1+d_2}{X_a})} - 1) \quad (4)$$

$P(\theta)$ must equal unity when integrated over solid angle. The extinction length for a given night will be the value of X_a where this condition is satisfied. Therefore, both the ground level phase function and scattering length may be extracted simultaneously from a near horizontal laser where a wide range of scattering angles are observed.

2.2.2 Orthogonal Measurement of Vertical Distribution

The above method can be applied to extract ground level parameters, phase function and mean scattering length. However, ground level parameters do not give enough information. On any two given nights that have the same ground level parameters the actual distribution of photons seen at the detector can be drastically different. A lack of information about the vertical distribution of aerosols is equivalent to knowing the type of material an attenuating optical element is made of, but not knowing how thick it is. Describing the vertical distribution is perhaps the most important and most difficult parameter to extract from the bistatic lidar data.

The vertical distribution, or change of the aerosol density with height, is proportional to how the reciprocal of the mean scattering length is changing with height. However, for the scintillation component of light emitted by an EAS, it is not important to know the exact concentration of aerosols or the exact scattering length at any given height. The necessary information is the transmission of the light at any given geometry through the atmosphere. Transmission of any geometry may be calculated given a single quantity as a function of height. This quantity is the integral of the reciprocal of the scattering length along a vertical path from the height at which the light originated to the point at which the light scattered. We will refer to this integral as vertical optical depth. This quantity is also known as aerosol optical thickness. If the laser goes from ground level to a height h with an elevation angle of α, and if we assume single scattering, the transmission of the laser can be given by:

$$T = e^{\frac{-1}{sin(\alpha)}\int_0^h \frac{\partial z}{X(z)}} \quad (5)$$

The optical depth, $\int_0^h \frac{\partial z}{X(z)}$, as a function of height is the information that we need from the vertical distribution. With this vertical optical depth we can calculate the transmission for any path that a cosmic ray or laser could take through the atmosphere, assuming horizontal uniformity.

To determine the optical depth we can begin by generalizing equation 4 for a laser at geometry i and photons received by detector element j

$$P_j = \frac{3}{16\pi}\frac{X_a(h_j)}{X_m(h_j)}(1 + cos^2(\theta_j))(R_{ij}e^{(\frac{1}{sin(\alpha_i)}+\frac{1}{sin(\alpha_j)})\int_0^{h_j}\frac{\partial z}{X(z)}} - 1) \tag{6}$$

Here α_i is the elevation angle of the source and α_j is the elevation angle at which detector element j viewed the photons. It is immediately obvious that this equation does not lend itself to a simple solution. In order to solve for the integral we would need information about the mean scattering lengths at specific heights and the phase function. We can only measure the phase function at ground level and it may change with height. Also, if we knew how the aerosol scattering length was changing with height we wouldn't need to measure the optical depth.

We can still gain useful information from this expression by changing the question that is asked. What can easily be determined is a lower bound to the amount of aerosols in the air. We know that the phase function must always be greater than or equal to zero. We may very easily calculate the smallest value that the integral could possibly have by assuming that the aerosol phase function is zero. This leads us to the expression:

$$\int_0^h \frac{\partial z}{X(z)}_{lowerbound} = ln(\frac{1}{R_{ij}})\frac{1}{\frac{1}{sin(\alpha_i)}+\frac{1}{sin(\alpha_j)}} \tag{7}$$

As was mentioned earlier the aerosol phase function is biased toward scattering in the direction of the incident radiation. If we only use data from a region where we expect the aerosol phase function to be close to zero, such as between 115 and 150 degree scattering angles, we can minimize the error in our lower bound.

The error in the lower bound for measurements made at a 120 degree scattering angle is shown in figure 2.2.1. The phase function was assumed to be the one shown in figure 1.1 and the molecular component of the atmosphere was parameterized with an $18km$ ground level scattering length and a scale height of $8km$. Figure 2.2.1 shows that as the scale height increases the percent deficit in the lower bound should not exceed approximately 25 percent. The deficit is also much lower than that for small scale heights, and becomes more accurate with distance above the ground. It should be noted that other models for aerosol phase functions predict less light at 120 degrees than the one used. This means that error in the lower bound due to a non zero phase function should not should exceed what is shown in figure 5 as long as the aerosol phase function near 120 degree scattering is not greater than 0.02. The percent error in the lower bound is not sensitive to the ground level scattering length.

It is important here to make a subtle point. One of the primary goals of the HiRes experiment is to determine if there is a flux of high energy cosmic rays above the GKZ limit. If the analysis of cosmic rays includes an over estimate of the amount of aerosol in the air the reconstruction will give a higher energy than the particle actually had. This could cause a lower energy particle to be mistakenly perceived to be above the GKZ limit. However, if a lower bound on the aerosol content where used in reconstruction the energy measured would be the lowest energy that the particle could possibly have. This, potentially, would leave no doubts as to whether or not a particle was above the GKZ limit. It should also be noted that even if multiple scattering significantly enhances the received signal the expression would still give a lower bound to the aerosol content. Generally,

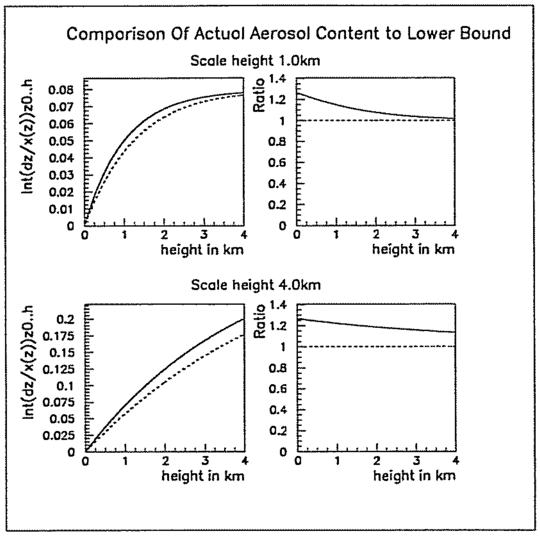

Fig. 2.2.1: This shows the error in the lower bound. The panels on the left show both the actual aerosol profile and the profile that would be measured using the lower bound technique. The panels on the right show the ratio between the actual profile and the expected lower bound measurement at a 120 degree scattering angle. A scale height of both 1 and 4 kilometers are shown. The ground level scattering length does not have a significant affect on the percent deficit in the lower bound.

the greater the received signal the smaller the concentration of aerosols. An enhanced signal due to multiple scattering would cause an underestimate of the aerosol content.

2.3 Global Fit of All Measurements

Including orthogonal measurements which are nearly model independent, a global fit for a specific model is also performed on the data. This global fit will assume that the number density of aerosols decreases exponentially with height and it horizontally uniform with no mixing layer at the ground. It also assumes that the composition and size distribution of aerosols remains constant with height above the ground. This assumption means that the normalized aerosol phase function will remain constant with height. The aerosol phase function is further constrained that it's value at large scattering angles cannot exceed half of the solid angle normalized molecular phase function.

The fit is performed for three parameters: ground level aerosol scattering length, exponential scale height, and two parameters to describe the phase function. The code which performs the fit is relatively simple. It steps across the parameters looking for a minimum in chisquare. When It finds a minimum, it zooms into the area around it and does finer stepping around that minimum until the parameters are determined to a sufficient precision.

2.4 Multiple Scattering Simulations (MCMSGDS)

Past analysis of fluorescence data assumed that photons were lost after their first interaction. This assumption effectively considers the atmosphere to be simply an attenuating medium. In an attenuating medium absorption occurs and photons truly are lost after their first interaction. However, at the wavelength of interest $\lambda = 355nm$ scattering is the dominant process in the atmosphere and allows the possibility for a photon to be measured after several interactions. It is possible for a photon to scatter multiple times, enter the detector, and be counted along with the single scattered signal.

How the multiple scattering enhancement might affect the signal can be determined using a very simple model of a halo growing around the beam as it travels through a medium. Suppose that a collimated beam is traveling through a scattering medium. Let y be the distance that it has traveled, N_o the original number of photons in the beam at $y = 0$ and $N(y)$ be the number of photons in the beam at y. Also, let $X(y)$ be the scattering length of the medium at y. If after a single interaction photons are truly gone (single scattering approximation) $N(y)$ will be:

$$N(y)_{ss} = N_o e^{-\int_0^y \frac{\partial r}{X(r)}} \tag{8}$$

However, some of the scattered photons will have small scattering angles. If the scattering angle is small enough it will virtually remain with the beam. Suppose that β is the percentage of light scattered from a point which can still be considered part of the collimated beam. Let $P_{z_{to}y}$ be the probability that one of these near axis photons scattered at z will make it to y without having a subsequent interaction. Then $N(y)$ would be given by:

$$N(y)_{ms} = N_o e^{-\int_0^y \frac{\partial r}{x(r)}} + \int_0^y \frac{\beta N(z)_{ss} P_{z_{to}y}}{x(z)} \partial z \tag{9}$$

The probability that a photon at z will make it to y is:

$$P_{z_{to}y} = e^{-\int_z^y \frac{\partial r}{X(r)}} \tag{10}$$

This yields the following expression:

$$N(y)_{ms} = N_o e^{-\int_0^y \frac{\partial r}{x(r)}} (1 + \beta \int_0^y \frac{\partial r}{x(r)}) \tag{11}$$

So, for this very simple model, the multiple scattering will cause the actual number of photons to be increased by a factor of 1 plus some constant multiplied by the optical depth. It should be noted that this simple model was given only as an example for what multiple scattering could do to the transmission.

To estimate the actual effect of multiple scattering on the data I developed a simulation program called MCMSGDS (Monte Carlo Multiple Scattering General Detector Simulation). A Monte Carlo is any simulation that makes use of random numbers. They are relatively simple to code and can quickly yield results to daunting calculations. Generally, they make use of analytic calculations to reduce the number of iterations that must be made.

In the development of MCMSGDS a decision was made to use as few analytic calculations as possible. This stipulation would have been unheard of a few years ago. However, computers today are fast enough to make this possible. Even with fast computers, this methodology is prone to computing times on the order of a week and low statistics. The reason for this decision was to dissolve all assumptions and simply find out what happens. The goal of MCMSGDS is not to calculate an exact answer to the question. It is meant to determine the approximate magnitude of the effect, the number of scatters which are significant, and to develop models and approximations that can be used in faster simulations.

The user is allowed to specify the aerosol content of the atmosphere, the direction of propagation, energy, and location of a laser source. In the interests of time the user should only use enough energy to produce sufficient statistics. This is usually on the order of $100pJ$ for $\lambda = 355nm$.

The path of the laser is cut into a series of small pieces. For each piece the number of photons scattering out is calculated. After this initial analytical calculation the simulation rely on random numbers. The simulation proceeds down the path of the laser photon by photon, piece by piece. A random number generator chooses a different direction for each photon to scatter in. The random directions come from the generation of two angles. The first is a uniformly distributed azimuthal angle around the direction of incidence. The second is the angle between the direction of incidence and the photons new direction. This comes from converting the uniformly distributed random variable from the generator into the distribution of the phase function at a given height. Once a direction has been chosen the photon travels a random distance to it's next scatter. This distance has a probability distribution based on the direction of the photon and the content of the atmosphere. This process continues on to ray trace every photon until it exceeds the maximum number of allowed scatters, reaches the boundaries of the simulation, or is measured by the detector.

The detector in the simulation is simply a spherical shell located at the origin. The radius of the shell is modified depending on how close the source comes to it. For nearby geometries, such as those used in phase function extraction, the radius is set to 30 meters. For geometries farther away the radius is set to 100 meters. As a photon crosses the surface of the sphere all relevant information, such as the number of times it scattered and incidence direction, is written to a file. Enough information is passed to the output in order to calculate anything we may wish to know about it. Cuts can be made on the multiply scattered data to approximate the effect on the actual detectors. For example, photons whose path lengths are too long or short to be included in the sample and hold time window are thrown out.

In the simulation the molecular component is approximated with an 17.2km mean scattering length (at $\lambda = 355nm$). This scattering length will change with λ^4 should the user alter the wavelength in the constants file. All vertical distributions are exponential decays. For the molecular component it has a mean height of 8km. All radiation is assumed to be unpolarized so the molecular phase function is $\frac{3}{16\pi}(1 + cos^2(\theta))$. The aerosols scattering length and mean height are varied by the user and the aerosol phase function is a trial function fit of the work done by Longtin. This phase function is shown in figure 1.1.

3 Results

The current data sample ranges a span of time from December 1999 to April 2001. Several hours of each night the detector was in operation the steerable laser system (HR2SLS) fired a pre-programmed sequence of shots. This sequence was designed to probe the aperture of the detector for atmospheric asymmetries and to determine aerosol parameters. The detector's response to one of these geometries is depicted in figure 3.1 below. Figure 3.1 shows which tubes received light from a particular laser geometry. This geometry has a long track in the detector and a wide range of observable scattering angles.

To analyze the data each cluster of photo-tubes must first be further divided or binned. This is done based on how the projection of the laser crossed the photo-tube cluster. For the near horizontal geometries, such as that shown in figure 3.1, each cluster is binned into four groups of tubes. Each group spans four degrees along the length of the laser track. The pointing direction of each group is found by a weighted average of the pointing directions of the tubes within it. For each group we may find the intersection in space of it's own pointing direction and the laser's incidence direction. This is the point in space where the single scattered light scattered toward the detector. Figure 3.2 shows these points for each laser geometry in the hourly sequence. This particular display of the data has been dubbed "The Spider Plot". Studies indicate that most of

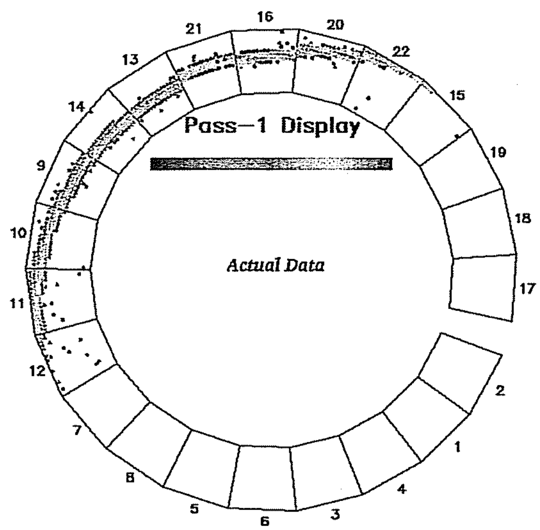

Fig. 3.1: The hires1 detector uses a real time event display which allows the operator to see the results of system triggers as they occur. Each square represents the photo-tube cluster associated with a mirror. Each pixel represents a tube which has received photons. The particular event displayed is a laser shot from hr2sls. This laser geometry is used to extract ground level scattering length and phase function.

the high energy cosmic rays will be observed within a $25km$ radius of the detector (AbuZayyad, 2000). Figure 3.2 shows that the laser system (HR2SLS) can probe much of the HiRes1 detector's aperture.

Information about aerosol content is determined by looking at the distribution of light received by the detector. There can be striking differences in this distribution when the aerosol content changes. Figure 3.3 shows data from two different days in the same month. The data is divided into four degree long bins. It is plotted on a log scale versus the total path length the light traveled. Variations in laser energy have been accounted for. As the path length of the light increases the amount of light seen from the beam generally decreases. When the aerosol concentrations are high this decrease occurs more rapidly. The aerosol content for a given night can be qualitatively ascertained by looking at distributions such as Figure 3.3. The acquisition of quantitative information will be discussed below.

3.1 Parameters Extracted in Single Scattering Approximation

The methods outlined above to extract aerosol parameters are dependent on the accuracy of a molecular prediction. They require a ratio of the distribution of light for an atmosphere with aerosols to one which is molecular. The molecular prediction for each geometry is extracted from data taken on a low aerosol day. The hourly data is paired with this molecular prediction and the ratio of their signals is calculated for each bin. Before we begin to apply these methods it is important to first check and see if low aerosol data is comparable to monte carlo simulation of a purely molecular night. Figure 3.4 shows data for a particular geometry on a low aerosol day. Overlayed on the data is the results of a monte carlo simulation for the same laser shot in a atmosphere without aerosols. The data is plotted on a linear scale. Black dots with statistical error bars denote the data while the molecular prediction is shown with circles. This figure shows

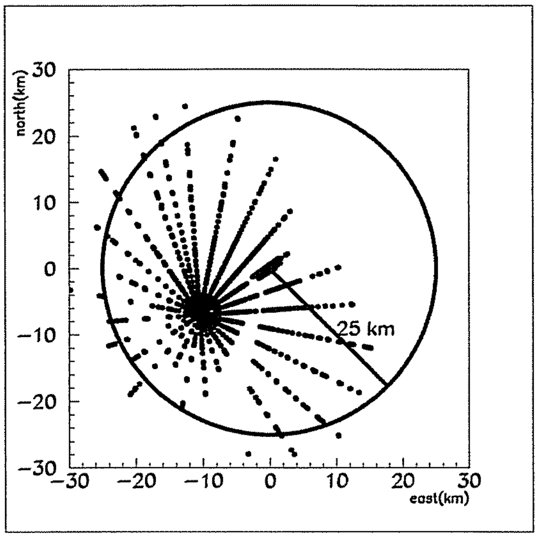

Fig. 3.2: This shows the points in space where light scattered from the laser and was measured by the detector. These are found by finding the intersection of the laser direction and the pointing direction of a group of photo-tubes. The detector is located at the origin. The laser system is approximately $7km$ south and $10km$ west of the detector. This has been dubbed "The Spider Plot".

that a low aerosol night is comparable to the molecular simulation.

The atmosphere during a given night can be qualitatively classified as low aerosol by two means. First the depolarization of polarized laser shots near the detector should be a minimum (polarization effects are discussed in the appendix). This is because an increase in aerosols increases the number of interactions and the possibility of depolarization. Second, the amount of light seen for large path lengths should be a maximum. This is because aerosols generally decrease the amount of light that can be detected over large distances. Third, the data should be free of evidence of clouds or haze layers. Clouds and haze layers will usually cause noticeable anomalies in the data.

3.1.1 Orthogonal Measurement of Ground Level Parameters

In the Methodology section of this paper the equation below was derived. This expression can be used to extract the aerosol phase function and ground level extinction length from laser data. The aerosol phase function is given in terms of the ground level extinction length and a ratio between the data in question and data from ideal conditions. This expression assumes the laser was near horizontal and close to ground level. Also, this expression assumes single scattering.

$$P(\theta) = \frac{3}{16\pi}\frac{X_a}{X_m}(1 + cos^2(\theta))(R(\theta)e^{(\frac{d_1+d_2}{X_a})} - 1) \tag{12}$$

It is possible to extract both the phase function and the extinction length because of the condition that $P(\theta)$ must be unity when integrated over solid angle. Before this method is applied to data it should be shown to be consistent with data where the aerosol concentration is known. The hires collaboration has a monte carlo simulation program that can predict detector response from lasers in different atmosphere conditions. The above method should be able to extract the phase function and the extinction length used by the simulation. Figure 3.1.1 shows the results of such a test.

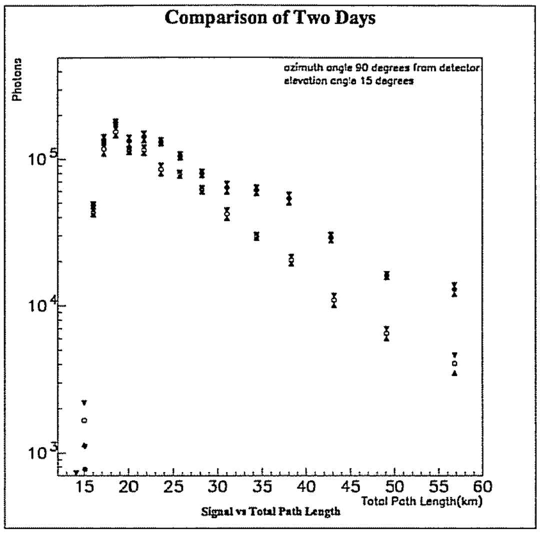

Fig. 3.3: This shows the distribution of light received by the detector for two different days at the same geometry. The data is binned into four degree wide sections of photo-tubes. It is shown on a log scale versus the total path length the light traveled. The data is from a geometry that is 90 degrees from the bisector between the laser and the detector and has a 15 degree elevation. There is a significant drop in the signal received on the second day. This is attributed to higher aerosol concentrations.

In order to determine these parameters a code searches for the extinction length that most closely normalizes the phase function. It is evident from the plot that the method correctly extracts the phase function from approximately 35° to 165° scattering angles. Though this is a significant portion of the phase function it is not enough to test for normalization.

Two versions of code were used on the data. The first version extrapolated the ratio of the signal to molecular expectation in order to determine the scattering length where normalization occurred. The ratio was fit to the form:

$$R(\theta) = Ae^{-B\theta} + C \tag{13}$$

An algorithm then proceeded to find the aerosol scattering length where the fit for the ratio produced a normalized phase function. In practice, this method worked well when aerosol concentrations were high. However, as aerosol concentrations begin to decrease this method can have problems. For example, on a day were the aerosols are virtually non existent the method will often find an aerosol scattering length of about 20km and a phase function which is nearly molecular. Though this solution fits the data from the horizontal shot as well as there being no aerosols, it is not consistent with the rest of the laser data. Also, small offsets in calibration or fluctuations in the data can sometimes lead to negative phase functions.

In order to get around these problem the range of possible phase functions that can be extracted has to be restricted from approaching molecular. In the above version of the code restricting the phase function properly proved to be difficult. To solve this problem An analytical function was created that predicted what the ratio should be for a given phase function and scattering length. This function was fit to the measured ratio by varying the scattering length and two parameters to describe the phase function. It was far more convenient to simply constrain the boundaries on the phase function parameters than to constrain the search for a scattering length that gave a

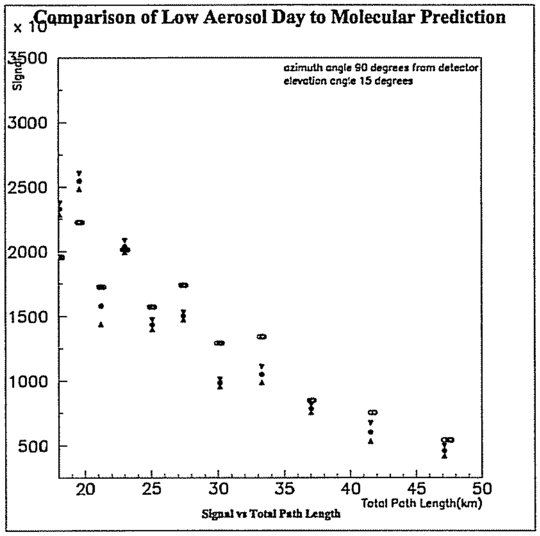

Fig. 3.4: This shows data from a low aerosol night superimposed on the results from a simulation with a molecular atmosphere. The data is denoted by black dots with statistical error bars and the simulation is shown by circles. This plot shows that low aerosol data is comparable to the molecular simulation.

normalized phase function for a given ratio. The phase function form that was used was obtained from the paper "Time-dependent Aureole About a Source in a Multiple-Scattering Medium" by E. Trakhovsky and U.P. Oppenheim. That phase function has the form.

$$P(\mu) = \frac{1-g^2}{4\pi}\left(\frac{1}{(1+g^2-2g\mu)^{3/2}} + f\frac{0.5(3\mu^2-1)}{(1+g^2)^{3/2}}\right) \tag{14}$$

$$\mu = cos(\theta) \tag{15}$$

This phase function is automatically normalized regardless of what g and f are. Though it may not be obvious by looking at the expression, the g parameter controls the forward peak of the phase function while the f parameter controls where and by how much the phase function turns back up past 100 degree scattering. Trakhovsky and Oppenheim give that a value of 0.7 for g and 0.5 for f should give a representative phase function in ultra violet wavelengths. For this fit g was allowed to vary between 0.3 and 0.95 while f was allowed to vary between 0.02 and 1.5. I will refer to this phase function parameterization as the ETUO phase function.

Rather than use a monte carlo simulation for the molecular prediction, data taken on a low aerosol night was used instead. The choice of using data rather than monte carlo decreases the chances that calibration errors will affect the measurement. However, there will be a problem if there is still a significant amount of aerosol even on days which we classify as low aerosol nights.

There are two geometries where this fit is attempted. They are both near horizontal geometries. One of these is on the northern side of the detector, the other is on the southern side of the detector. These geometries are symmetric to one another. The separation in space between these two geometries is less than 1km. The scattering lengths and phase functions extracted from these shots individually should be identical. Figure 3.1.2 shows the scattering length extracted on the southern side of the detector versus the scattering length extracted on the northern side of the detector.

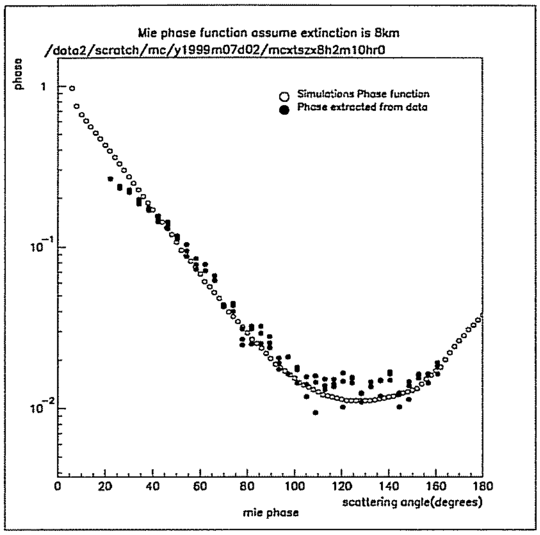

Fig. 3.1.1: This figure shows the phase function that was extracted from the simulated data. Overlayed on it is the phase function that was programmed into the simulation. This phase function was found at the correct aerosol scattering length 8.0km.

Below 10km scattering lengths the extracted parameters are nearly identical for the two sides. Beyond 10km the difference begins to grow until the limits of the fit, 150km, is reached. The sensitivity to the measurement decreases quickly as scattering length increases. Recall from the introduction that the scattering length is equal to the reciprocal of the product of the scattering cross section and the number density of aerosols ($x = \frac{1}{\rho\sigma_{scat}}$). So, rather than plotting the correlation of the scattering lengths it should be more meaningful to see the correlation of the reciprocal of the scattering lengths for the two sides of the detector. Figure 3.1.3 shows the correlation of the reciprocals.

The spread of the reciprocal of the scattering lengths on the two sides of the detector remains more constant as the reciprocal changes than does the spread in the scattering lengths.

The average effect of the aerosols at ground level can be found by taking the average of the reciprocal of the scattering length. The reciprocal of that average will give the ground level aerosol scattering length which is, on average, applicable to the atmosphere above the hires detectors. For the northern side of the detector the average reciprocal of the scattering length is $0.034km^{-1}$ and for the southern side is $0.038km^{-1}$. This yields that the average scattering length for both sides of the detector is approximately $28km$. These distributions are shown in figures 3.1.4 and 3.1.5.

This analysis also must determine the phase function in order to find the ground level scattering length. Figure 3.1.6 and 3.1.7 show the average phase function for the two different sides of the detector. Because sensitivity to the phase function quickly decreases as the scattering length increases only measurements where the scattering length is below 30km and greater than 10km are used. Scattering lengths below 10km are not included in this average because these ultra high aerosol concentrations may have sources with low scattering albedos.

In each plot the average for that side is shown with black dots and the phase function from Longtin, the standard desert model, is represented with circles. The normalized molecular phase function is also represented for comparison. The northern average is very close to an ETUO phase function with parameters $g = 0.77$ and $f = 0.84$. The southern average is very close to an ETUO phase function with parameters $g = 0.75$ and $f = 0.84$.

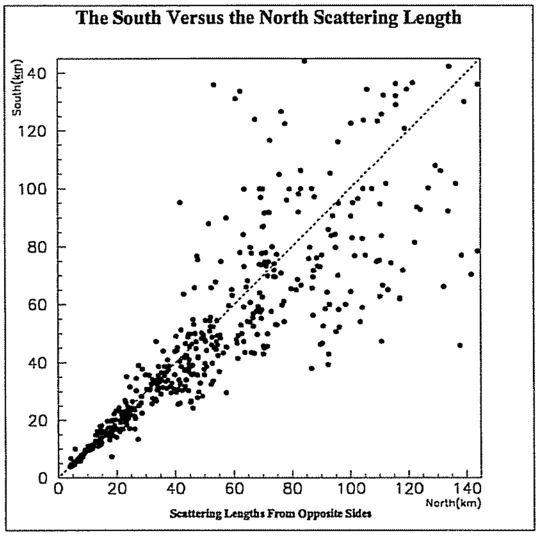

Fig. 3.1.2: This figure shows the ground level scattering length extracted from the southern side of the detector versus the scattering length extracted from the northern side of the detector.

3.1.2 Orthogonal Measurement of Vertical Distribution

In the methodology section of this paper the below formula was derived to obtain a lower bound on the vertical optical depth of the aerosols.

$$\int_0^h \frac{\partial z}{X(z)}_{lowerbound} = ln(\frac{1}{R_{ij}}) \frac{1}{\frac{1}{sin(\alpha_i)} + \frac{1}{sin(\alpha_j)}} \tag{16}$$

The normalization that was used in the analysis came from a low aerosol day rather than the monte carlo. The reason for doing this was to remove possible systematic effects from the detector calibration. This formula was applied to find the aerosol vertical optical depth from ground to a height of $3.5km$. This was done by taking an average of all of the lower bounds measured between 3 and 4km for a given hour.

Before showing the distribution of the optical depth for the data set it is instructive to review the assumptions that led to the lower bound. The assumptions were that the atmosphere was horizontally uniform, which is assumed in all techniques, and that aerosol scattering was negligible at the height of measurement.

It can be shown that the atmosphere has a reasonable degree of horizontal uniformity by looking at correlations between optical depths measured by symmetric geometries. The geometries at 109 degrees azimuth and 319 degrees azimuth at a 15 degree elevation are symmetric shots that reach up to 4km above the ground. These two geometries are both 75 degrees in azimuth from the bisector between the laser and the detector. At a height of 3.5km the geometries are separated by approximately 26km. Figure 3.1.8 shows the correlation between optical depths measured at different portions of the atmosphere.

The other assumptions that go into the lower bound is that aerosol scattering is negligible at the point of measurement. This means that the light scattered toward the detector was predominantly from molecular scattering. The lower bound could be as much as 30% lower than the actual optical depth if the scale height and aerosol phase function are both large at the scattering angle of observation. However, for scale heights less than 2km the lower bound should be within 10% of

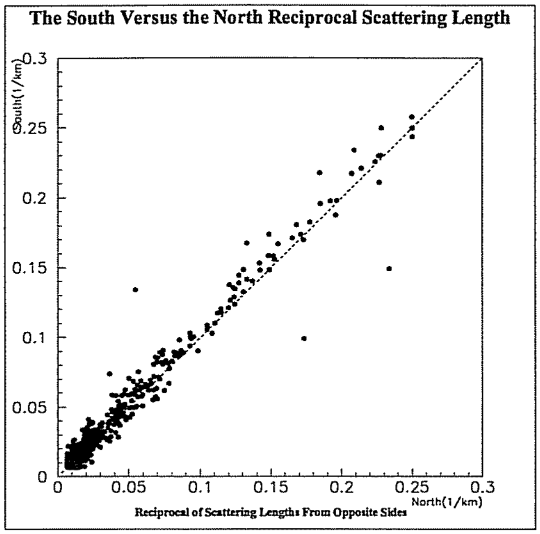

Fig. 3.1.3: This figure shows the reciprocal of the ground level scattering length extracted from the southern side of the detector versus the reciprocal of the scattering length extracted from the northern side of the detector.

the actual optical depth. Figure 3.1.9 shows the distribution of the hourly measurements of the average vertical optical depth from ground to between 3 and 4km. The negative values correspond to instances when the amount of light received was greater than what was expected for a molecular atmosphere. This might mean that the night chosen as our molecular base line may not quite be molecular. This could also be caused by clouds or haze layers. If the laser hits the cloud or haze layer it could cause much more light to scatter toward the detector than would do so in a molecular atmosphere. It should be noted that if the laser goes behind a cloud or haze layer without directly hitting it, much less light will get to the detector than on nights with dense, well behaved aerosol distributions.

3.1.3 Global Fit of All Measurements

A global fit was also performed on all of the data. This fit assumed that the aerosol number density decreased exponentially with height and that the aerosol phase function and cross section remained constant with height. The phase function used in the fit is the same two parameter phase function as is used in the orthogonal measurement of phase function and scattering length, the ETUO phase function.

$$P(\mu) = \frac{1-g^2}{4\pi}\left(\frac{1}{(1+g^2-2g\mu)^{3/2}} + f\frac{0.5(3\mu^2-1)}{(1+g^2)^{3/2}}\right) \tag{17}$$

$$\mu = cos(\theta) \tag{18}$$

The fitting routine steps across the parameter space looking for the combination of 4 aerosol parameters (scattering length, scale height ETUO g and f) that have the smallest chisquare. The range of possible values of the scattering length are restricted to be within a range that will yield physical results for a given hour. This range of physical scattering lengths is found by looking at the average value of the ratio of the near horizontal shots between 110 and 140 degree scattering

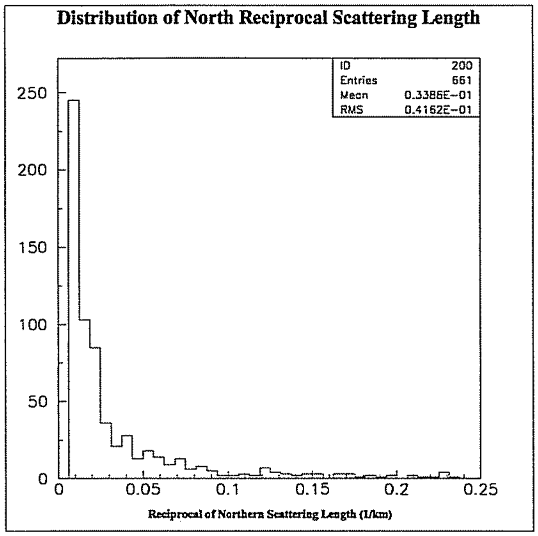

Fig. 3.1.4: This figure shows distribution of the reciprocal of the ground level scattering length extracted from the northern side of the detector. The average of this reciprocal is $0.034km^{-1}$. This corresponds to a scattering length of $29km$

angles. The maximum possible scattering length is then found by assuming that the aerosol phase function is zero in the 110 to 140 degree scattering region. If the phase function where non zero then a shorter scattering length would give the same ratio in this region. This assumption and equation (4) yields the simple expression:

$$X_{aerosol\_Maximum} = \frac{-14.0km}{log(R_{110,140})} \tag{19}$$

In this expression the total distance traveled by the light is said to be $14km$. It is actually closer to $13.5km$. By using $14km$ the maximum possible scattering length is overestimated slightly. This is intentionally done to slightly broaden the range of possible scattering lengths.

The minimum possible scattering length is calculated by assuming a maximum value for the aerosol phase function. The assumption was that the aerosol phase function could not, in this scattering region, exceed half of the molecular phase function. This is found by solving the following transcendental equation with a binary search:

$$\frac{P_{aerosol}}{P_{molecular\ maximum}} X_{molecular} + X_{aerosol\_Minimum}\left(1 - R_{110,140} e^{\frac{10.0km}{X_{aerosol\_Minimum}}}\right) = 0 \tag{20}$$

In this expression the total distance traveled by the light is said to be $10km$ rather than 13.5. This is done intentionally to slightly broaden the window of possible scattering lengths. It should be noted that maximizing the ratio between the aerosol and molecular phase functions in this region to 0.5 is a restriction based on the fit rather than on physics. Without this restriction it would be possible for near molecular data to masquerade as data with aerosols that have a molecular like phase function.

The following geometries are included in the global fit (azimuth,elevation): (36.0,0.6), (32.0,0.6), (102.3,15.0), (109.0,15.0), (319.0,15.0), (124.0,15.0), (124.0,10.0), (304.0,15.0), (304.0,10.0). The first two geometries are the near horizontal shots that are used to determine the phase function.

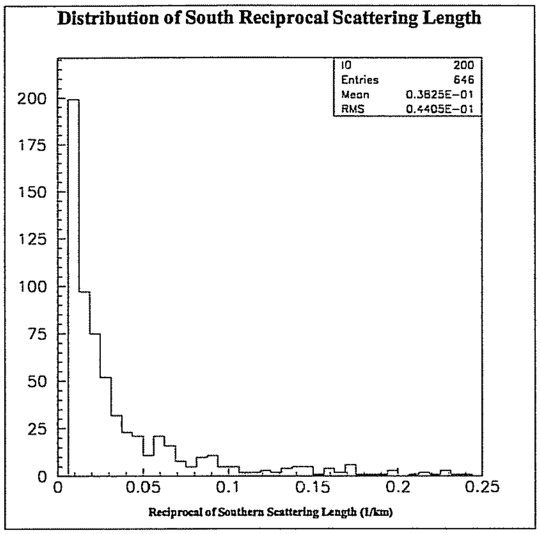

Fig. 3.1.5: This figure shows the reciprocal of the ground level scattering length extracted from the southern side of the detector. The average of this reciprocal is $0.038 km^{-1}$. This average corresponds to a scattering length of $26 km$

The other geometries are elevated shots that reach up to 4km above the ground. They were chosen because the ratio between regular data and data on a near molecular day resembled analytic predictions. It should be noted that there are some geometries that do not look like either analytic predictions or monte carlo predictions.

Measurements made near ground level are assigned a 5% uncertainty. The uncertainty decreases linearly with height so that it is 2.5% uncertainty at $4 km$ above the ground. This extra weighting of the measurements made higher in the atmosphere helps the fit to find the proper scale height.

The fit goes through three passes. The first pass is a "Global" pass. The second pass is a "Phase" pass. The third pass is a "Scale" pass. In the global pass 40 scattering lengths are chosen between the boundaries; 40 scale heights are chosen between 0.05km and 4km, 4 f's are chosen within it's boundaries as well as 4 g's. The global pass looks over all geometries included in the fit and tries every combination of these parameters. The combination of parameters that resulted in the smallest total chisquare is then passed to the second pass or phase pass.

In the phase pass of the fit the scale height is fixed and only the near horizontal geometries are considered. A much finer search is then performed to find the scattering length and phase function. This new search is centered around the parameters found in the global pass. The range about these parameters in this pass is one sixth the range considered in the global pass. This range is divided up into 30 pieces in both the scattering length and the phase function parameters. Every combination is considered to find the one with the smallest chisquare.

The final pass is the scale pass. In this pass the phase function parameters and scattering length obtained in the phase pass are used and kept fixed while the scale height is allowed to vary. In this pass the near horizontal shots are excluded. The scale height is allowed to vary within plus or minus 0.25km of the value reached at the end of the global pass. In this range 100 scale heights are tested to see which one, with the parameters from the phase pass, results in the smallest chisquare from the elevated shots.

Once this scale height has been found a chisquare is calculated where every point is weighted with 5% error regardless of height. This is the chisquare that is used to determine how good a

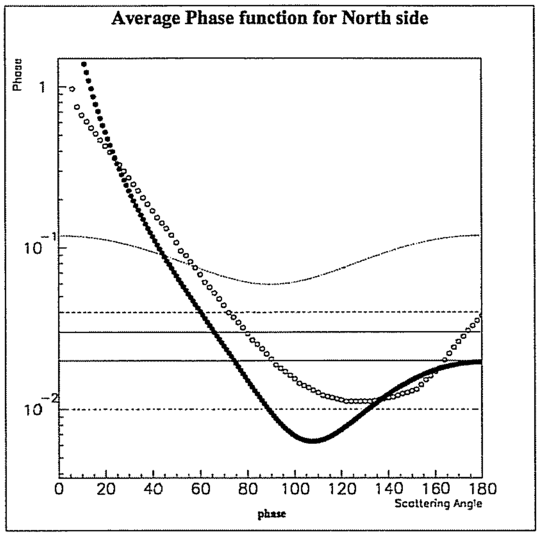

Fig. 3.1.6: This figure shows the average phase function extracted for the north side of the detector with black dots. The standard desert or Longtin phase function is shown with circles. The molecular phase function is shown with a dotted line. This average only included days where the ground level scattering length was greater than 10km and less than 30km. This average phase function is approximately a ETUO phase function with $g = 0.77$ and $f = 0.84$

given fit was.

Figure 3.1.10 shows the correlation between the vertical optical depth at 3.5km predicted by the fit and the vertical optical depth from the lower bound technique.

Figure 3.1.11 shows the distribution of the vertical optical depth at 3.5km calculated from the fit parameters. There is a sharp drop at zero because it is not possible to have parameters that will give a negative optical depth. The average optical depth at 3.5km is approximately 0.04. The plot excludes hours where the chisquare was greater than 10.0 and the number of points in the measurement was below 100. Since the errors are not particularly well understood, and not necessarily Gaussian, a chisquare of less than 10.0 still gives an acceptable fit. Chisquares of 20 or greater are usually the result of the laser hitting a cloud. Fits where the Chisquares are between 10 and 20 are ambiguous. It is possible that there may simply be one bad point. If these fits are used they should be individually looked at to visually decide if the data is salvageable.

Figure 3.1.12 shows the distribution of the total vertical optical depth calculated from the fit parameters. For the exponential distribution this total optical depth is simply the ratio of the scale height and the ground level scattering length. The mean is approximately 0.05.

Figure 3.1.13 shows the reciprocal of the ground level scattering length. The mean reciprocal of the aerosol scattering length is $0.046km^{-1}$. This corresponds to a ground level scattering length of approximately $22km$.

An important question to be asked is whether or not there is a correlation between the scale height of the aerosols and the ground level scattering length. There is not a direct correlation between the ground level scattering length and the scale height. However, there does appear to be a correlation between the range of possible scale heights and the reciprocal of the ground level scattering length. Figure 3.1.14 shows the scale height versus the reciprocal of the ground level scattering length. For reciprocals greater than $0.1km^{-1}$ or scattering lengths smaller than $10km$ the scale height never extends past $0.7km$. As the aerosol concentration decreases at ground level

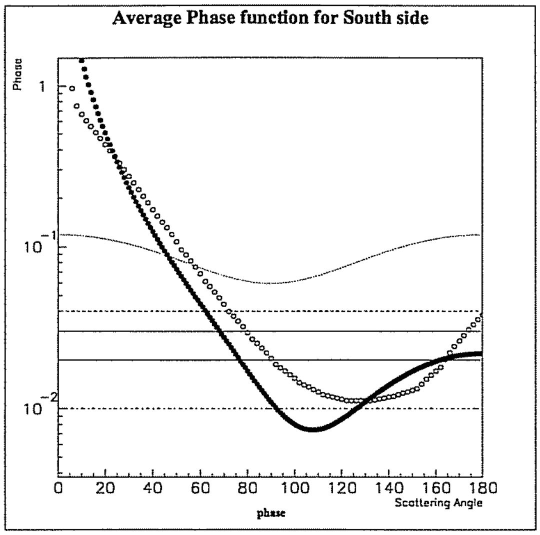

Fig. 3.1.7: This figure shows the average phase function extracted for the south side of the detector with black dots. The standard desert or Longtin phase function is shown with circles. The molecular phase function is shown with a dotted line. This average only included days where the ground level scattering length was greater than 10km and less than 30km. This average phase function is approximately a ETUO phase function with $g = 0.75$ and $f = 0.84$

the range of possible scale heights increase to be within the full range of the fit. This is partially due to the fact that at low aerosol concentrations it becomes increasingly difficult to determine exactly how many of them there are or how high up they go. For very low aerosol concentrations the fit may settle on any scale height with more dependence on the fluctuations in the data than in the aerosol concentration. However, tests of the fitting procedure suggest that such a break down in parameter resolution cannot entirely account for figure 3.1.14. It should be noted that though the fit will have difficulty determine a scale height when aerosol concentrations are low it would not have such a difficulty when they were high. If there were larger scale heights at smaller scattering lengths the fit would definitely indicate that. So, figure 3.1.14 does show that when ground level scattering lengths are below $10km$ the aerosols are most likely to have a small scale height below $0.7km$. It also shows that when ground level aerosol concentration is low, or the scattering length larger, there is a much greater range of possible scale heights even if scale heights found for very long scattering lengths cannot be trusted.

The global fit also extracts a phase function. The average phase function of nights with acceptable chisquares and scattering lengths between $10km$ and $30km$ is shown in figure 3.1.15. This average phase function can be described with an ETUO phase function parameterization with $g = 0.70$ and $f = 0.83$.

From all of this one can determine an average aerosol concentration for the atmosphere above the hires detectors. Because large scale heights are less meaningful if the aerosol concentration is low, an average scale height should be found by weighting each scale height with the reciprocal of the scattering length. This gives an average scale height of about $1.1km$. So the average aerosol optical properties in the single scattering approximation at $355nm$ can be described with a scattering length of $22km$ a scale height of $1.1km$ and a phase function described with an ETUO parameterization with $g = 0.70$ and $f = 0.83$.

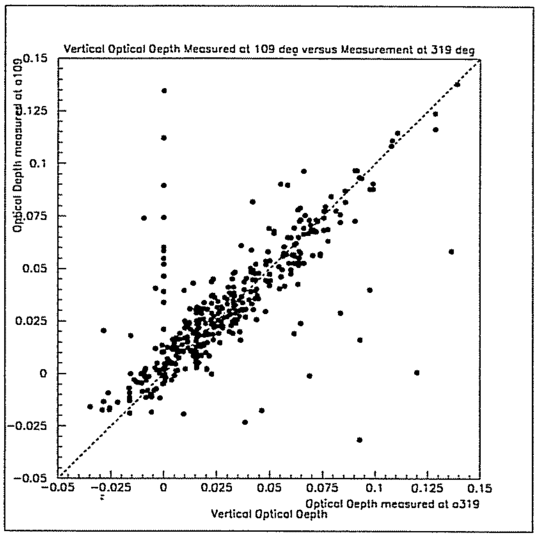

Fig. 3.1.8: This figure shows the optical depth measured at one geometry versus the optical depth made at a symmetric geometry.

3.2 Multiple Scattering Results

MCMSGDS was ran for many geometries with many different aerosol parameters. However, due to problems with low counting statistics a small set of these simulations are actually useful. These are shots in a near horizontal geometry and shots at 15degree elevation with an azimuth of 30 degrees from the bisector between the laser and the detector sphere.

The results of MCMSGDS were used to validate a simple multiple scattering model and provide approximate values for parameters in that model. The simple halo model given in the methodology section of the paper is a bit too simple to actually use. In order for it to be useful it must take into account the fact that at the solid angle which is effectively part of the beam at a point y decreases along the beam as one over the distance from the point y squared. If this is taken into account the transmission of a collimated beam in a medium can be approximated as:

$$N(y)_{ms} = N_o e^{-\int_0^y \frac{\partial r}{X(r)}}\left(1 + \int_0^y \frac{A}{(y-r)^2}\frac{\partial r}{X(r)}\right) \tag{21}$$

The above equation assumes that the phase function is more or less constant over a patch of solid angle around the beam at y. Photons scattered into this small patch of solid angle have effectively remained with the beam. This assumption will not be good when r in the second integral in the above equation is very close to y. So the second integral should not be taken all the way to y.

First, the simplest possible aerosol distribution is a uniform one with a constant scattering length throughout the medium. If y is far from the point of origin of the collimated source, $y >> 0$, and if the second integral is integrated only up to $y - \delta$ where $\delta << y$ then the multiple scatter transmission for a uniform atmosphere is:

$$N(y)_{ms} = N_o e^{-\int_0^y \frac{\partial r}{X(r)}}\left(1 + \frac{1}{X(r)}\frac{A}{\delta}\right) \tag{22}$$

Therefore, the percent increase of the signal due to multiple scattering enhancement, for this model, will be proportional to the scattering length of the medium. This model then suggests that

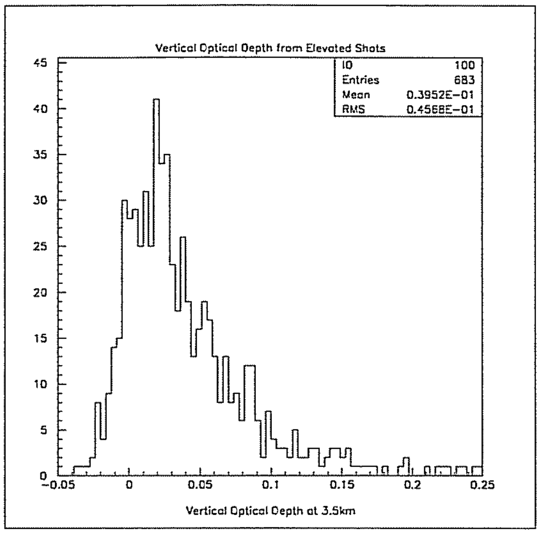

Fig. 3.1.9: This figure shows a histogram of hourly average of the vertical optical depth at 3.5km measured with geometries with 15 and 10 degree elevations.

once a halo has developed the relative magnitude between the halo and the unscattered portion of the beam remains constant. The constant $\frac{A}{\delta}$ should depend on the detector being used and should have some dependence on the aerosol phase function.

The next case to be considered is a collimated beam in a medium where the aerosol scattering length is decreasing exponentially in one direction of the three dimensional space. This is similar to how we expect the scattering length of aerosols to actually change. We expect that the scattering length should decrease exponentially with height. This case is actually fairly difficult to do analytically. However, numerical integration shows that in this case also the multiple scattering enhancement is proportional to the inverse of the scattering length at the point of measurement.

So, suppose the atmosphere has an exponentially decreasing distribution of aerosols. If a collimated beam travels to a height H above ground, then light scattered at this height is received back at the ground the expected signal will be proportional to:

$$Sig = N_o e^{-(\frac{1}{sin(\alpha_1)}+\frac{1}{sin(\alpha_2)})\int_o^H \frac{\partial z}{x(z)}}(1+\frac{1}{x(H)}\frac{A_{out}}{\delta})(1+\frac{1}{x(0)}\frac{A_{in}}{\delta}) \tag{23}$$

It should be noted that A_{in}, or the halo constant for the incoming portion of the lights path, should be virtually zero. If the point of scatter is far from the detector then the solid angle around the point of scatter where multiply scattered light can still be imaged with the single scattered light is fairly large. However, the solid angle of the light collector at the end of the return path is much smaller. This means that the halo on the return path will likely not be imaged by the detector. So the above expression would reduce to:

$$Sig = N_o e^{-(\frac{1}{sin(\alpha_1)}+\frac{1}{sin(\alpha_2)})\int_o^H \frac{\partial z}{x(z)}}(1+\frac{1}{x(H)}\frac{A_{out}}{\delta}) \tag{24}$$

The above model is based on the idea that the multiply scattered photons which enter the detector come from a halo built up around the beam. There are other trajectories that multiply scattered photons can take and still enter the detector. The above model will be used only to approximate and parameterize the results of MCMSGDS.

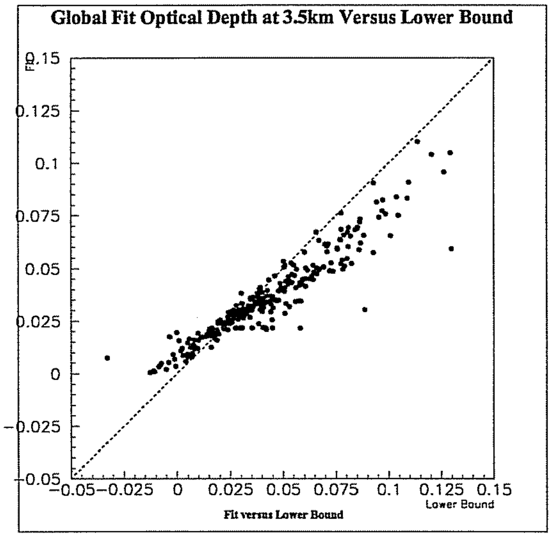

Fig. 3.1.10: This figure shows the correlation between the vertical optical depth at 3.5km calculated with the fit parameters with the lowest chisquare versus the vertical optical depth obtained via the lower bound technique.

As it turns out, the results of MCMSGDS are easily parameterized with the above model. With a near horizontal geometry the simulation was performed with 35,30 25,20,15,10, and 5km scattering lengths with large scale heights. This is virtually the same as if there were a uniform scattering length. Cuts were placed on the singly and doubly scattered photons that reached the detector in an attempt to more closely resemble the actual hires detectors. These cuts were on the geometry of the entering photons and on the path length differences between singly and multiply scattered photons. The sum of the doubly scattered photons with scattering angles between 24 and 156 degree which passed these cuts where divided by the sum of the singly scattered photons. This was plotted versus the inverse of the scattering length in the simulation. Figure 3.2.1 shows the results. A linear fit has a slope of .899km and an intercept of 0.017. The intercept should, of course, correspond to the multiple scattering enhancement caused by molecular scattering. In this simulation the molecular component has a ground level scattering length of 17.2km. This means that the multiple scattering enhancement constant for molecular scattering, 0.292km, is approximately one third of the aerosol multiple scattering enhancement constant.

$$\frac{(0.017)(17.2km)}{(0.899km)} = 0.325 \tag{25}$$

Before using these results great care must be taken. This particular geometry takes relatively little time to simúlate sufficient statistics because it passes so close to the ground and the detector. For these same reasons the magnitude of these corrections cannot be used for any other geometry. First of all, some of the scattered photons that may have contributed to the measurement were deleted from the simulation by the ground. Also, because the geometry was so close to the detector there is an unknown number of multiply scattered photons that could not be imaged at this distance but may be able to be imaged at further distances from the detector.

The above simulation does tell us the relative magnitude of multiple scattering introduced by a molecular phase function and the multiple scattering that would be introduced by a forward peaked or aerosol phase function. This needs to be known when looking for the multiple scattering

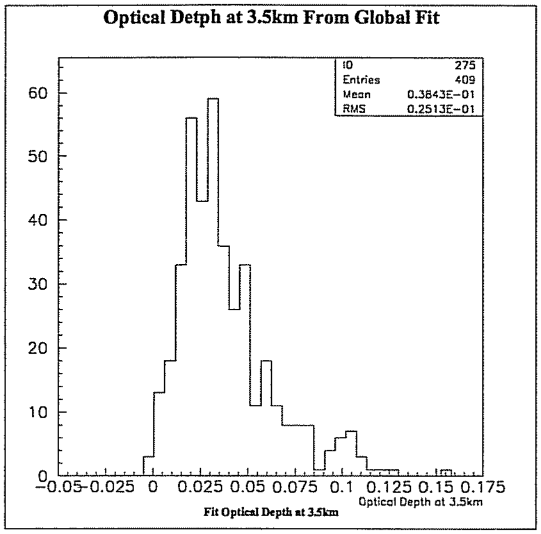

Fig. 3.11: This figure shows the distribution of vertical optical depth at 3.5km calculated from the fit parameters. The mean optical depth is approximately 0.04.

enhancement of elevated shots farther from the detector.

The simulation was also run at a 15 degree elevation and 30 degrees azimuth from the bisector between the laser and the detector. These simulations were run with the following aerosol parameters (scattering length, scale height): (30km,1km),(20km,1km),(14km,3km),(10km,3km),(7km,3km). This data was also binned and cut to approximate the hires detectors. Also, only bins where the statistical error was below 20 percent were allowed. The percent enhancement due to multiple scattering was plotted versus the reciprocal of the aerosol scattering length plus 0.33 multiplied by the reciprocal of the molecular scattering length. The results of this simulation gave a multiple scattering halo constant of 3.84+/-0.4km. They are plotted in the figure 3.2.2.

3.2.1 Global Fit of All Measurements with Multiple Scattering Corrections

A global fit was also performed on all of the data with multiple scattering corrections. This fit assumed that the aerosol number density decreased exponentially with height and that the aerosol phase function and cross section remained constant with height. The transmission of light through this atmosphere came from the results of the halo model from the above multiple scattering section. In this fit the transmission of light for the near horizontal shots was determined by:

$$T(H,\alpha_1,\alpha_2) = e^{-(\frac{1}{sin(\alpha_1)}+\frac{1}{sin(\alpha_2)})\int_o^H \frac{\partial z}{x(z)}}(1+\frac{0.899}{x_a(H)}+\frac{0.27}{x_m(H)}) \tag{26}$$

The transmission for elevated shots farther from the detector was determined by:

$$T(H,\alpha_1,\alpha_2) = e^{-(\frac{1}{sin(\alpha_1)}+\frac{1}{sin(\alpha_2)})\int_o^H \frac{\partial z}{x(z)}}(1+\frac{3.84}{x_a(H)}+\frac{1.27}{x_m(H)}) \tag{27}$$

The outgoing elevation angle is α_1. The incoming elevation angle is α_2. The height where the light scattered is given by H.

Due to personal time constraints the global fit with multiple scattering corrections was only performed on the data taken in the year 2001. Currently this corresponds to 5 months of data.

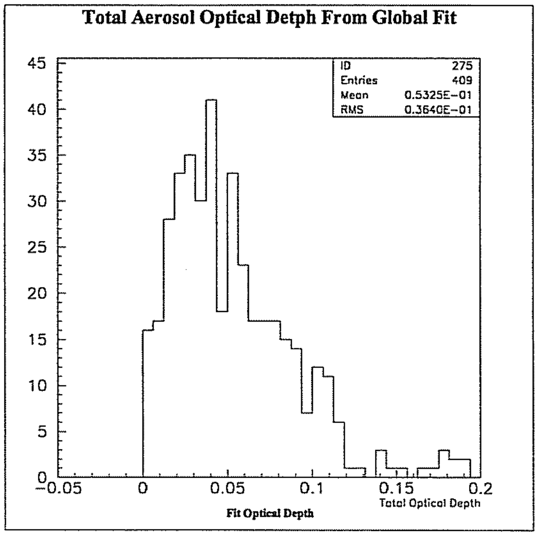

Fig. 3.12: This figure shows the total vertical optical depth calculated from the fit parameters. The mean total optical depth is approximately 0.05.

After cuts on chisquare and the number of points in the fit there were 108 measurements in this set which originally contained 214. The distribution of the reciprocal of the scattering length is given in figure 3.2.3. The distribution of total optical depth is given in figure 3.2.4. The average phase function is given in figure 3.2.5. The average scattering length corresponds to approximately $21km$. The average total optical depth is 0.055. The average phase function has ETUO parameters of $g = 0.76$ and $f = 0.73$. Because of the limited data set it is difficult to draw conclusions from these results.

4 Discussion and Conclusion

In this paper methods to extract aerosol parameters were discussed. These parameters were extracted using data from a bistatic lidar at $355nm$ consisting of a steerable laser system (hr2sls) and the High Resolution Fly's Eye Hires1 detector. Aerosol parameters were extracted assuming single scattering using the ratio between data and the expected signal from a purely molecular atmosphere. This molecular signal was obtained from data taken on a very clear day.

There was also an attempt to apply multiple scattering corrections to the aerosol parameters. These were based on a simple "halo" model of multiple scattering that was fit to the results of a simulation program called MCMSGDS. Due to personal time constraints the multiple scattering corrections and there effects have not yet been fully explored.

Based on the parameters extracted in the single scattering approximation the average optical properties of the aerosols above the Hires detectors at dugway was determined. Using the global fit, this average atmosphere at $355nm$ was a ground level scattering length of $22km$ and a scale height of $1.1km$. The average phase function was an ETUO parameterization with a $g = 0.70$ and $f = 0.83$. The average optical depth at $3.5km$ above the ground from the global fit was consistent with the average lower bound. The average scattering length and phase function extracted independent of data from heights greater than .2km has a longer average scattering length and slightly different average phase function.

This average scattering length and phase function are in conflict with the standard desert

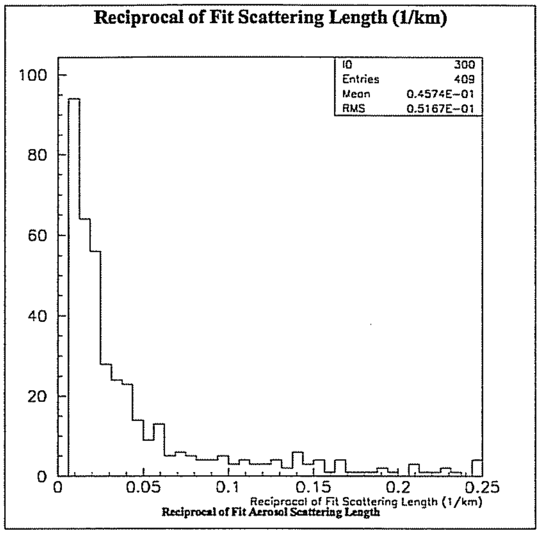

Fig. 3.1.13: This figure shows the distribution of the reciprocal of the ground level scattering length extracted in the global fit.

model. The parameters extracted from the data suggest that the aerosol concentration above the Hires dectectors is approximately half of what the standard desert model suggests. This is not too surprising because the air at Dugway proving ground is supposed to be exceptionally clear. There were also differences between the measured phase function and the standard desert or Longtin phase function. This could stem from two possible sources. The first possibility is that the parameterization chosen for the phase function is, for some reason, not acceptable. The second possible source of difference is that Longtin's phase function is a calculation based on measured indices of refraction for a wavelength of $550nm$. The phase function extracted here is at a different wavelength, $355nm$, and is a direct measurement rather than a calculation. It is possible that the longtin phase function is simply not applicable to this experiment.

The use of these average aerosol properties rather than the Standard dessert model will significantly reduce the reconstructed energies of distant cosmic ray air showers and have a significant effect on the ultra high energy cosmic ray spectrum. More work needs to be done to validate these aerosol parameters and the methods for obtaining them.

5 References

AbuZayyad, T. Z. (2000),*The Energy Spectrum of Ultra High Energy Cosmic Rays.* (Doctors Thesis). University of Utah.

CRC Handbook of Chemistry and Physics,72,14-12 (1991)

Elterman L. and Toolin R.W.. (1965). Atmospheric Optics. Handbook of Geophysics and Space Environments, Chapter 7.

Greisen K. (1966). *End To The Cosmic Ray Spectrum.* Physical Review Letters. Volume 16, Number 17:748-750

Longtin David R., Shettle Eric P., Hummel John R., Tryce James D. (1988). *A Wind Dependent Desert Aerosol Model.* (Technical Report). Air Force Geophysics Laboratory: AFGL-TR-88-0112

Martin G., Mathews J. A. J. (1999). *Analysis of Time Variant Molecular Atmosphere for the Purpose of Air Fluorescence Measurements.* Pierre Auger Project Note: GAP-99-XYZ

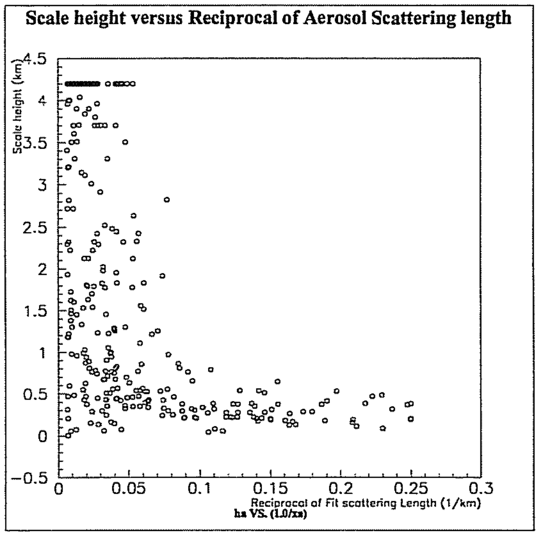

Fig. 3.1.14: This figure shows the fit scale height versus the reciprocal of the fit ground level scattering length. As the scattering length increases (smaller reciprocal) the range of possible scale heights increase.

Mumford J.R. (1999). *Steerable Laser System For the High Resolution Fly's Eye.* ICRC99 conference proceedings.

Mumford J.R. (2000). *Atmospheric Horizontal Uniformity Measured by a Steerable Laser System at the High Resolution Fly's Eye.* Senior Honors Thesis, The University of Utah.

Sokolsky P. (1989) *Introduction to Ultrahigh Energy Cosmic Ray Physics.* (Addison-Wesley Publishing Company, Inc., Redwood City, California).

Trakhovsky E., Oppenheim U. P. (1983). *Time-Dependent Aureole About a Source in a Multiple Scattering Medium.* APPLIED OPTICS, Volume 22, No. 11.

University of Utah HiRes Ultra High Energy Cosmic Ray Group (1997-2001). Personal Communication.

Zatsepin, G. T., Kuz'min, V.A. 1966, Soviet Phys.-JETP Lett.,4,78

6 Appendices

6.1 Scattered Light From Polarized Laser Shots

Through this analysis the laser shots that have been used were generated with circularly polarized light. The shot pattern of hr2sls also includes linearly polarized laser shots. The polarization of the beam is changed by using quarter wave plates which are within an automated filter wheel. The scattered light measured by the detector can change drastically depending on the orientation of linearly polarized light relative to the scattering plane. Though this effect has not been exploited in the analysis it is a very important aspect of molecular scattering when performing a side scattering laser experiment.

I will briefly go over the derivation of the molecular scattering phase function and cross section and then will show that the hr2sls data is consistent with predicted polarization effects. The differential scattering cross-section for light scattered by the atmosphere can be calculated analytically by assuming the constituents are dielectric spheres. Rayleigh or molecular scattering is calculated

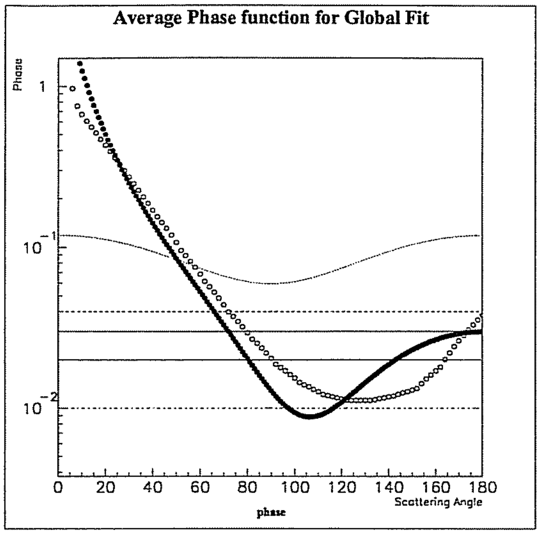

Fig. 3.1.15: This figure shows the average phase function of the aerosols obtained from the global fit. The average phase function is shown with black dots. The standard dessert (Longtin) phase function is shown with circles. The molecular phase function is also plotted with a dotted line for comparison. This average is approximately an ETUO phase function with parameters $g = 0.70$ and $f = 0.83$

in the limit that the sphere is small enough compared to the wavelength of the incident radiation that the electric field vector is the same magnitude and direction throughout the extent of the sphere. Light is scattered by this sphere through the mechanism of dipole radiation.

In Jackson's Classical Electrodynamics (1975) the scattered electric field due to an induced dipole is derived. Assuming that the magnetic moment is insignificant the scattered field is:

$$\vec{E_{sc}} = -\frac{1}{\lambda^2}\vec{p}\frac{e^{ikr}}{r} \tag{28}$$

The wavelength of the incident radiation is λ. The distance from the scatterer is r and the dipole moment of the scatterer is $\vec{p}$. The power radiated from the scattered field in some direction, per unit solid angle per incident intensity is the differential scattering cross section. Since the intensity is the electric field squared, the differential scattering cross section becomes:

$$\frac{\partial\sigma_{scat}}{\partial\Omega} = r^2\frac{|\epsilon_{scat}\cdot\vec{E_{sc}}|^2}{|E_{inc}|^2} = \frac{1}{\lambda^4 {E_o}^2}|\epsilon_{scat}\cdot\vec{p}|^2 \tag{29}$$

Here ϵ_{scat} is the unit vector pointing in the direction of the scattered electric field. Jackson gives us that the dipole moment of a dielectric sphere in a constant electric field is:

$$\vec{p} = a^3\vec{E_{inc}}\frac{(\mu-1)}{(\mu+2)} \tag{30}$$

Here, a is the radius of the sphere and μ is the dielectric constant of the medium. Placing the above expression into the one prior to it the following will represent the differential scattering cross section of incident radiation on the sphere.

$$\frac{\partial\sigma_{scat}}{\partial\Omega} = \frac{a^6}{\lambda^4}\frac{(\mu-1)^2}{(\mu+2)^2}|\epsilon_{inc}\cdot\epsilon_{scat}|^2 \tag{31}$$

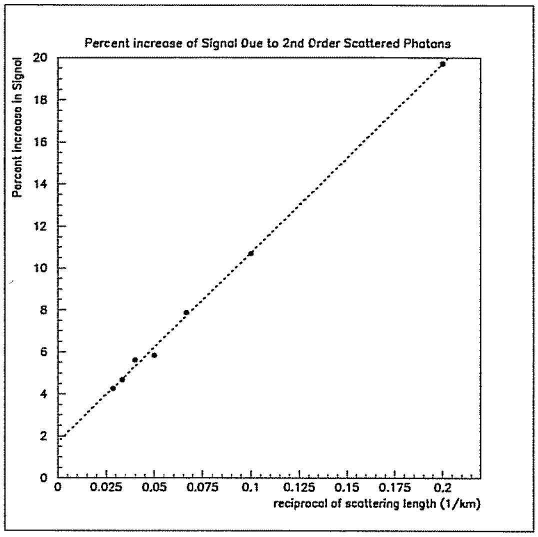

Fig. 3.2.1: This figure shows the percent multiple scattering enhancement for a horizontal geometry as a function of the inverse of the scattering length. The linear fit has a slope of 0.899km and an intercept of 0.017.

The above shows that the scattering cross section is inversely proportional to the wavelength to the forth power, λ^4. This is the explanation for why the sky is blue. Blue light has a smaller wavelength so it is scattered more by the air molecules. Also, the differential scattering cross section is proportional to the dot product of the unit vectors of the incident and scattered electric fields.

We define a coordinate system where θ is the scattering angle and ϕ is the angle from the vector perpendicular to the scattering plane to the direction of the incident polarization. The molecular phase function (solid angle normalized differential scattering cross section) for linear polarized light is then:

$$P_{molec}(\theta) = \frac{3}{16\pi}(sin^2(\phi)cos^2(\theta) + cos^2(\phi)) \tag{32}$$

Consider the above equation. If the incident polarization is in the scattering plane then the phase function will be proportional to $cos^2(\theta)$. If the incident polarization is perpendicular to the scattering plane then the phase function will be constant with scattering angle.

When the laser is steered to the near horizontal orientation a test of the above is performed. The polarization is changed to be nearly perpendicular to the scattering plane and to be nearly parallel to the scattering plane. The ratio of the data in the parallel orientation to data taken in the perpendicular orientation is very close to $cos^2(\theta)$. See figure.

If we average over the possible polarizations, which is valid for circularly or randomly polarized light, and then renormalize over solid angle we return to the form of the molecular phase function used in this analysis.

$$P_{molec}(\theta) = \frac{3}{16\pi}(cos^2(\theta) + 1) \tag{33}$$

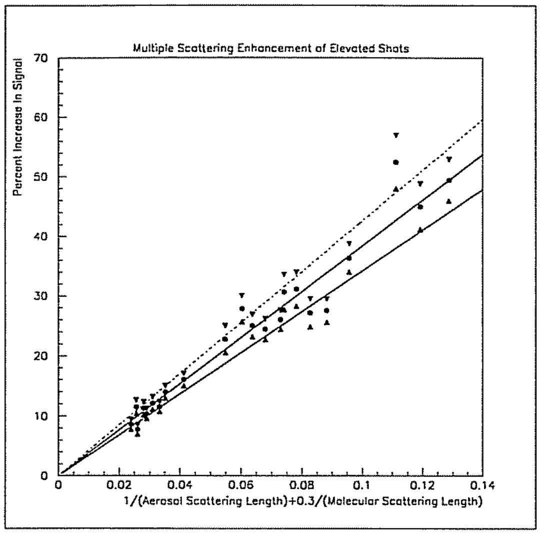

Fig. 3.2.2: This figure shows the percent multiple scattering enhancement for a 15degree elevated geometry. The relative magnitude of molecular multiple scattering to aerosol multiple scattering was assumed to be the same as in the horizontal shots. The multiple scattering halo constant for aerosols was 3.84+/-0.4km.

6.2 MCMSGDS Documentation

Due to time constraints (I'm leaving today) this documentation will have to be brief. The program mcmsgds is in the hires soft dst2k libraries. This program performs a photon by photon simulation of either a laser or cosmic ray. The point of this simulation is to determine the effect of multiple scattering. The usage statement of this program should be sufficient to describe how to input command line parameters to simulate cosmic rays and lasers at whatever geometry or aerosol content desired. There is a version of the program on my chpc accounts that uses mpi. I do not have time to check it into the libraries as well. However, all it does is set up a different seed and different file for each processors and then allows them to work independently. The same could be achieved by using the version that is now in the libraries as a separate process with a different seed on each processor.

Keep in mind, of course, that this is a photon by photon simulation. It would not be wise to put the full energy of these sources into the simulation. If you do your job will take 50 years. Needless to say you would need special permission from the folks at chpc to run a job for that long. Only put in enough energy so that sufficient statistics can be reached. For laser simulations use 100-2000x 10^{-12} Joule depending on how far away the laser is and how big you allow the detector dome to be. A 100pj simulation will probably not take more than a day or two on an unburdened pentium processor. For more than that you will need to set it off on multiple processors with different seeds. For cosmic rays you will need at least 40x $10^{-}6$ Joule. Cosmic ray simulations tend to take longer.

The program outputs a text file called hrtemp.dat. This file can be converted to an rzed binary file using the program A2RZmcmsgds. This program is, of course, also in the dst2k libraries. This rzed file will have the following variables in it with the following meanings.

(pxo,pyo,pzo) These variables indicate the location of the photon at it's first scatter or where it was emitted in the case of an EAS.

(pxl,pyl,pzl) These variables indicate the location of the photon before it entered the detector

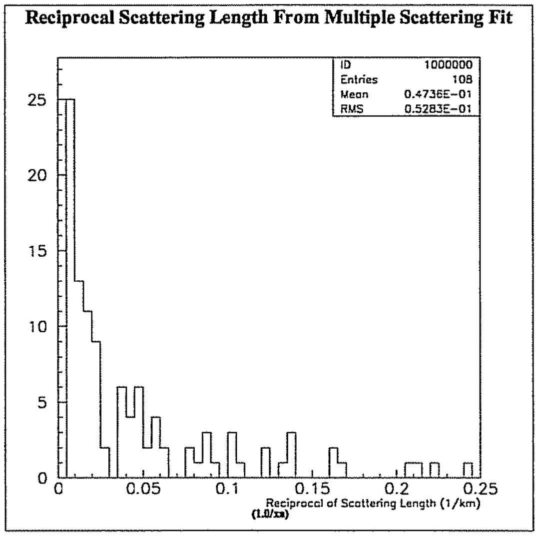

Fig. 3.2.3: This figure shows the distribution of the reciprocal of the scattering length for the limited data set where the fit with multiple scattering corrections was performed. The average is $0.047km^{-1}$. This corresponds to a ground level scattering length of approximately $21km$.

dome.

(sx,sy,sz) These variables indicate either the location of the laser or the core location of the shower.

(usx,usy,usz) These variables indicate the unit vector describing the direction of the track or laser.

(pux,puy,puz) These variables indicate the unit vector describing the direction of the photon as it entered the detector sphere.

(nscat) This variable indicates the number of interactions with the atmosphere that the photon has had. Note that in the case of an EAS emission from the shower is considered scattering by the atmosphere.

(pathlngt) This variable is the total path length that the light has traveled. Keep in mind that this path length is from (sx,sy,sz) to point of scatter to next point of scatter... to detector.

(sener) This is the source energy.

(ha,xa) the scale height and scattering length of the aerosols.

(stype) This variable indicates the type of photon that it was. If stype is 1 then it means that this photon came from a laser. If stype is 2 I believe that it means this is a fluorescence photon and if stype is 3 it is from cherenkov radiation.

(xcross,ycross,zcross) these variables tell where on the detector dome the photon crossed through.

(xmax,xo) These variables tell the depth of shower maximum and the depth of first interaction of an EAS if an EAS was simulated.

6.3 ATMBIN:Laser Data Binning Program for Atmospheric Analysis

A major part of doing the atmospheric analysis is binning the data. Initially this was done with a program called hr2slslsrprof. This first program had serious limitations and was replaced. The new program was called atmbin.

The atmbin code works on either real or monte carlo data. Since the methods outlined in the

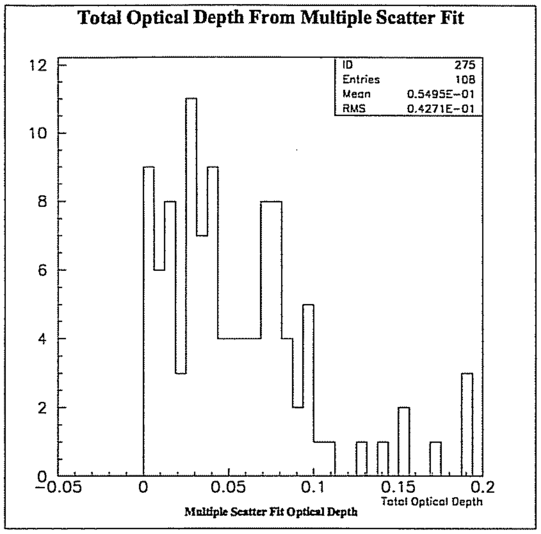

Fig. 3.2.4: This figure shows the distribution of the total aerosol optical depth calculated from parameters from a global fit with multiple scattering corrections.

above paper require a molecular prediction the atmbin program can match data to what is predicted for a molecular atmosphere. Throughout most of this work this molecular prediction came from a monte carlo. The program has either a one file mode or a two file mode. The one file mode simply bins data without matching to a molecular prediction. The two file mode (one file a molecular prediction) processes two files and then puts the results of both into output for further analysis. Also, in two file mode it will only include tubes that triggered in the molecular prediction and below the point of qdcb saturation. It is also supposed to flag a bin if a tube did not trigger that did in the molecular prediction. It should be noted that due to problems with memory, two file features are only available for a select set of shots. These set of shots are set in atmbin_mapfill.f. All other shots will be treated the same as in single file mode.

The main function of the code is written in C, in atmbin.c. This main function is simply used for string manipulation of the command line. Once command options have been determined they are passed to a fortran function, in atm_bin.f. The rest of the program is written in fortran.

The main fortran function,atm_bin.f, processes one of the input dst files at a time. It is passed a variable called fnum in order to determine whether it is working with the molecular normalization file or the data file. For the most part things are done the same regardless. The main difference is that when a call is made to write to the output the data will be written to arrays in a common block rather than to the users choice of output. Then, when it is actually working on the data the numbers stuffed into the common block are written with the data output.

The first thing atmbin does is to read in an event from the dst file and check to see which banks are available. The availability of banks which are key to the analysis are stored in variables in the common block tstbnk. For example tstbnk_sls2, tstbnk_hbar. These variables will be 1 if the bank is available and 0 if it is not. The program then reads in information about the event from generic functions such as atm_nmir, atm_tr_udir, atm_tr_loca. The function atm_nmir gets the number of mirrors in event. The function atm_tr_udir gets the unit vector direction of the track from the source in hires1 coordinates. The function atm_tr_loca gets the location of the tracks source. Other functions get the energy of the event and other information identifying it's geometry, source, and the detector it was seen in. These generic functions report the requested values from whatever bank

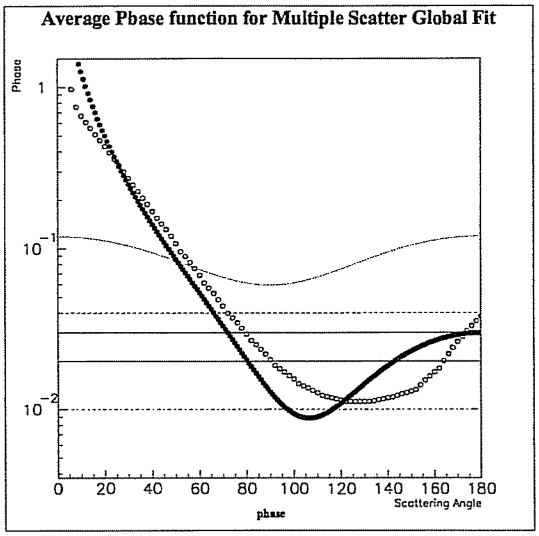

Fig. 3.2.5: This figure shows the average phase function from the limited set with multiple scattering corrections.

is most appropriate. Therefore, in theory, the atm_bin.f main function should be easily modified to work with any detector or known source.

Once the program has information about the geometry of the track it may then bin the data from each tube. Atmbin cuts each mirror into either 1,2,4, or 8 bins depending on command line options. The default is 4 bins per mirror. Each tube is given a further designation called an order. Each tube is assigned and order and bin based on the geometry of the track and how it crosses the mirror. Atmbin was originally able to bin a track in either up down bins, left right bins, and in both diagnol lines of symmetry. It chose a method of binning, or map, depending on how the track crossed the mirror. If a track went straight up and down through the mirror then bins would be made of the left right rows of the cluster. If the track went from left to right in the cluster the bins would be made of the up and down rows. Also, if a track went diagnolly through the cluster the bins would be made of the diagnols going in the opposite direction. This was so that a single program could effectively bin a track regardless of how it crossed a mirror. However, due to bugs that were found and have yet to be resolved as of the writing of this thesis the diagnol binning has effectively been disabled. This leaves the program using only up down and left right binning.

Besides a bin a tube is also given an order. Order indicates the angle between a tubes pointing direction and the surface of the track detector plane. A tube is designated as being within order 1 if the angle from the plane is less than 1 degree. A tube is designated as order 2 if it is less than 3 degrees from the plane. A tube is designated as order 3 if it is less than 5 degrees from the plane. If a tube is greater than 5 degrees from the plane then it is ignored. It should be noted that a given order contains all of the tubes within the lower orders. For a track far from the detector the increase in the amount of light seen in a bin with increase in order will likely be from multiple scattering. The definition of order 1,2, and 3 can be changed at the command line but the above mentioned limits are the default settings.

The program will create output data for the average value of each bin for each set of shots with the same orientation and filter. It is possible, at the command line, to limit the maximum number of shots in an average. By default the average will include all consecutive shots with the same settings as long as they all take place within a time span of six minutes or less. The length of this

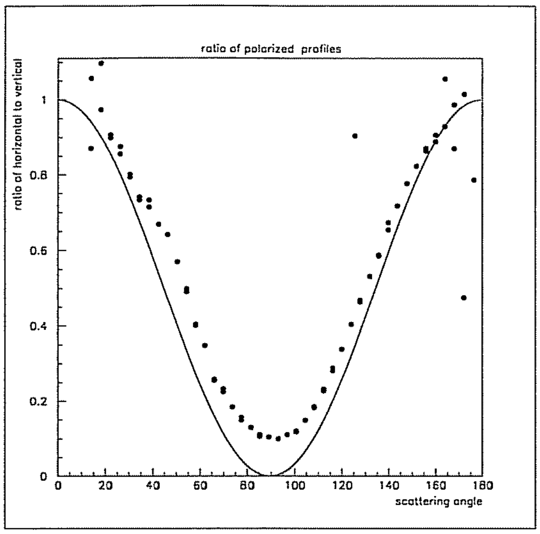

Fig. 3.6.1: This figure shows the ratio data taken in the near horizontal geometry with two different polarizations. Data taken with the polarization parallel to the scattering plane is divided by data taken with the polarization perpendicular to the scattering plane. The result is the predicted $cos^2(\theta)$ as predicted by dipole scattering from small dielectric spheres.

time span can be altered by changing the TDIFF variable in the atm_bin.inc file.

The binned and averaged data is written to ntuples in a binary file of rz or rzed data format using the -rz command line option. These files can be read into paw using the histfile 0 file.rz command. The rz file is opened using the atmbin_openrz.f function. The rz file is written to using the atmbin_writerz.f function. All output files are closed using the atm_clseout.f. Originally the program was intended to be able to create rz, text, dst, and or pbm (pixel bit map) output. The pixel bit map would have been an image of the atmosphere based on the laser data input. However, as of the creation of this documentation it is actually only able to produce rz output. It should not be difficult to add the ability for other forms of output if they are desired by the user. Functions to create these other forms of output should be called from atm_openout.f, atm_write.f , and atm_clseout.f.

Currently the output is automatically called hrtemp.rz. The user should rename this file after it has been created. Variables in the ntuple are as follows:

event: This holds the event number of first shot in the average

hraw: This variable is equal to 1 if the user forced use of the hraw1 bank using command line option -hraw1

jday: This is the julien day the event occured on according to the definition of Julian day in hraw1 bank.

hr: This is the hour that the event occurred calculated from the decimal Julian day in the hraw1 bank.

minute: This is the minute that the event occurred calculated from the decimal Julian day in the hraw1 bank.

nshots: This is the number of shots that has been included in the average.

azi: This is the azimuth angle of the laser in hires1 coordinate system. It should be in degrees.

zen: This is not the zenith angle. This is the elevation angle of the laser. We started with a bad naming convention but we have chosen to stick with it. This is elevation angle in degrees.

dg0: This is the definition of the angle at which order1 ends.

dg1: This is the definition of the angle at which order2 ends.

dg2: This is the definition of the angle at which order3 ends.

energy: This is the average energy sent to the sky for a set of shots.

energysqr: This is the average energy squared sent to the sky for a set of shots.

sradian: This is the scattering angle between the incident direction of the laser and the pointing direction of the bin. This is given in radians.

d1: This is the distance from the source to the point at which the light scattered toward the bin. This is calculated by finding the point of closest approach (intersection) of the vector pointing out from the bin and the vector of the lasers direction. The function atm_dist performs this calculation.

d2: This is the distance from the point at which the light scattered toward the bin to the detector. Note that $d1 + d2$ is the total path-length of the laser. This is calculated by finding the point of closest approach (intersection) of the vector pointing out from the bin and the vector of the lasers direction. The function atm_dist performs this calculation.

xint: This is the east coordinate of the point at which light scattered toward the bin. The origin is the port'a potty at hires1. This is calculated using d1, the location of the laser, and the direction of the laser.

yint: This is the north coordinate of the point at which light scattered toward the bin. The origin is the port'a potty at hires1. This is calculated using d1, the location of the source, and the incident direction of the laser.

zint: This is the distance above hires1 at which light scattered toward the bin. This is calculated using d1, the location of the source, and the incident direction of the laser.

xt: This is the x component of the unit vector of the bin. It is calculated by a signal weighted average of the pointing directions of the tubes in the bin.

yt: This is the y component of the unit vector of the bin. It is calculated by a signal weighted average of the pointing directions of the tubes in the bin.

zt: This is the z component of the unit vector of the bin. It is calculated by a signal weighted average of the pointing directions of the tubes in the bin.

phtn: This is the average number of photons in the bin for a given set of shots. The photons come from the hraw1 bank if hbar is not available. If hbar is available it will only use hraw1 bank if the user enabled the -hraw1 option at command line.

phtnsq: This is the average number of photons in the bin squared for a given set of shots. Can be used to get standard deviation of phtn.

phtnpmj: This is the average number of photons in the bin divided by the energy sent to the sky. phtnpmj is equal to photons per mili joule.

phtnpmjsq: This is the average number of photons in the bin divided by energy sent to the sky squared. Used to get standard deviation of phtnpmj.

norm: This is the average number of photons in bin divided by energy sent to sky for the dst file which was supplied for a molecular prediction. If no molecular prediction will be zero.

normsq: This is the average number of photons in bin divided by energy sent to the sky squared for the dst file which was supplied for a molecular prediction. If no molecular prediction will be zero.

bin: This is the number of the bin in the mirror.

order: This is the order of the measurement.

mirror: This is the mirror where measurement was made.

ntubes: This is the average number of tubes that were in a given bin and order.

filter: This is the filter that was placed in front of the source during the measurement.

smap: This is a number indicating how the mirror was binned. If it is 0 then left right bins were used. If it is 10 then up down bins where used. If it is +1 or -1 then diagnol binning was used.

tdc: Indicates the relative time that the tubes triggered.

flag: Should be greater than zero if something bad happened. "Bad" things include a tube not triggering that should have.

As of the writing of this documentation this program was only able to deal with events from the hr2sls and data from hires 1. However, it should not be difficult to add other sources to the program as long as the events are matched with and identifying bank. Below I will list aspects and functions called by atm_bin.f that would need to be modified in order to allow for atmbin to process other combinations of data.

Some things are in place for the possibility of taking data from two detectors and multiple sources. Below is a list of functions that need to be modified in order to add detectors and sources. Next to the function or file is an explanation of what needs to be done.

1. atm_bin.inc: First this file will need to have the variable NVAR increase by 2. This is the maximum number of variables in the ntuple. Also the atm common block should have two variables added. One to indicate detector and one for source. Currently in the output it is assumed that hires1 is detector and that hr2sls is source.

2. atmbin_openrz.f: This function needs to have two more variables out to the output ntuple. One should indicate what the light source is. The other should indicate which detector saw the light. Also add to the tstbnk common block banks for hires2 and banks to identify the new sources you wish to look at.

3. atmbin_writerz.f: Modify this so that it will write out the two variables mentioned above.

4. atm_tstbank.f Modify this so that it will test for banks and store whether or not it found important ones.

5. atm_nmir.f Modify so that it can return number of mirrors in event from hires2 banks.

6. atm_tr_udir.f Modify this so that it will return the unit vector of the track in space of whatever other sources you wish to add.

7. atm_tr_loca.f Modify this so that it will return the location of the origin of the source you wish to add.

8. atm_dt_loca.f Modify this so that will return the location of hires2 in hires1 coordinates if banks indicative of hires2 are present.

9. atm_getplane.f Modify this so that it will calculate track detector plane based on pointing direction and location of source if plane fit is not available.

10. atm_get_time.f Modify this so that it will get time from hires2 banks if they are available.

11. atm_get_fnum.f Modify this so that it can get filter number from hr1sls or roving laser if it's banks are available. Or, perhaps, some property such as which flasher is being seen.

12. atm_mkbin.f This is a function that designates each tube with a bin and an order. It does this by looking at the tube directions and normal of the track detector plane. However, it is using geoh xvtube, yvtube, and zvtube to get the tubes pointing directions. Obviously this will not do for hires2. There are two places in the code where it uses these functions. Make it so that in the event that hires2 is the detector of choice it will use what is appropriate to get out the tube pointing vectors.

13. atm_getntube.f Modify this so that it will return the total number of tubes in event if hires2 banks are present.

14. atm_get_energy.f Modify this so that it will return the esky energy of hr1sls if it's banks are available, or that of the roving laser. Or have it return 1.0 if it is a flasher or some other source where we do not know shot to shot variation in energy.

15. atm_indxmir.f Modify this so that it can get mirror number of tube regardless of detector.

16. atm_indxtube.f Modify this so that it can get mirror tube number of tube regardless of detector.

17. atm_indxdet.f Modify this so that it will set the detector index to 2 if banks indicative of hires2 detector are in event.

18. atm_getphtn Modify this so that it can return photons from hires2 detector as well as hires1 depending on available banks.

19. atm_gettdc Modify this so that it can get tdc from hires2 as well as hires1.

7 Acknowledgements

I would like to acknowledge all of those at the High Resolution Fly's Eye Cosmic Ray Group at the University of Utah as well as collaborators. I would specifically like to thank my supervisor Lawrence Wiencke for allowing me to follow my ideas and my instinct while keeping me from going off on fruitless tangents. I would also like to thank Charlie Jui for originally offering me this position at the High Resolution Fly's Eye in 1997 (in the JFB men's room after one of his classes).